

Nanotribology and Nanomechanics of MEMS/NEMS and BioMEMS/BioNEMS Materials and Devices and Biomimetics

**Prof. Bharat Bhushan
Ohio Eminent Scholar and Howard D. Winbigler Professor
and Director NLBB**

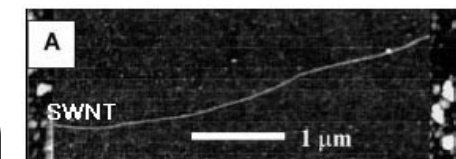
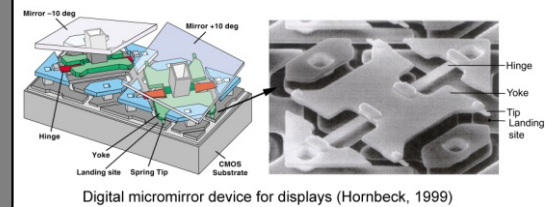
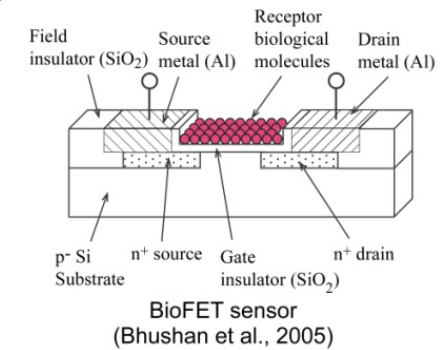
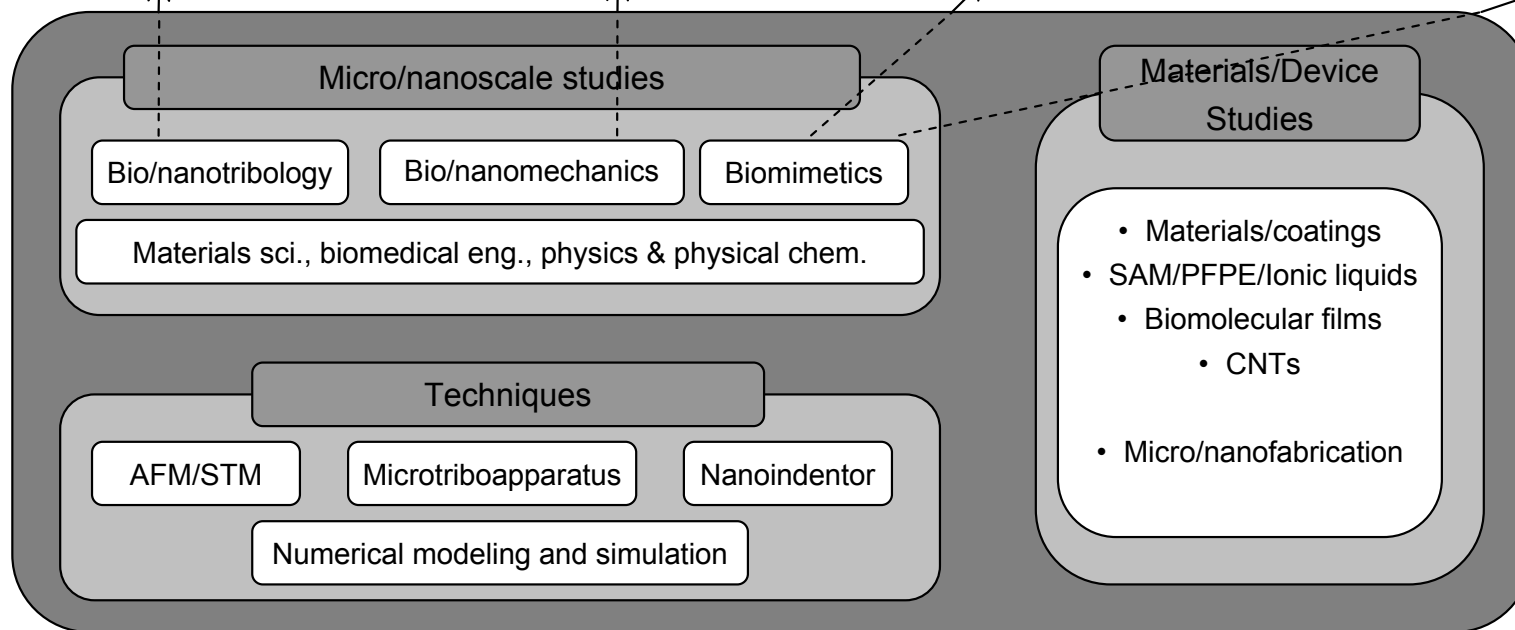
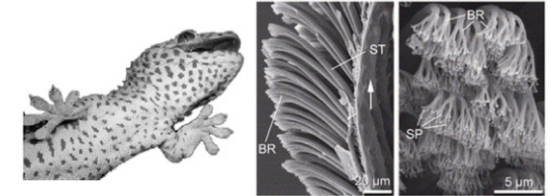
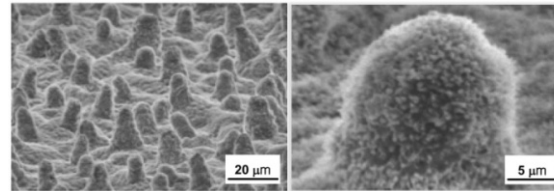
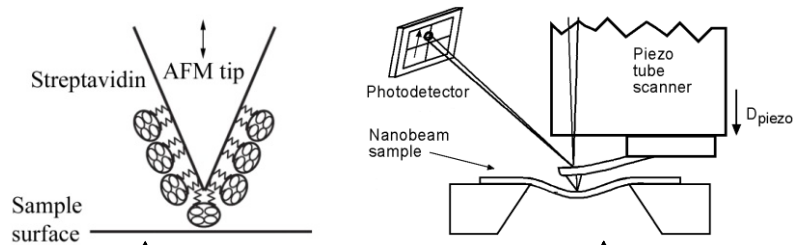
Bhushan.2@osu.edu

Nanoprobe Laboratory for Bio- & Nanotechnology and Biomimetics

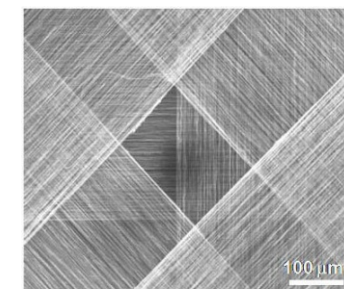


© B. Bhushan

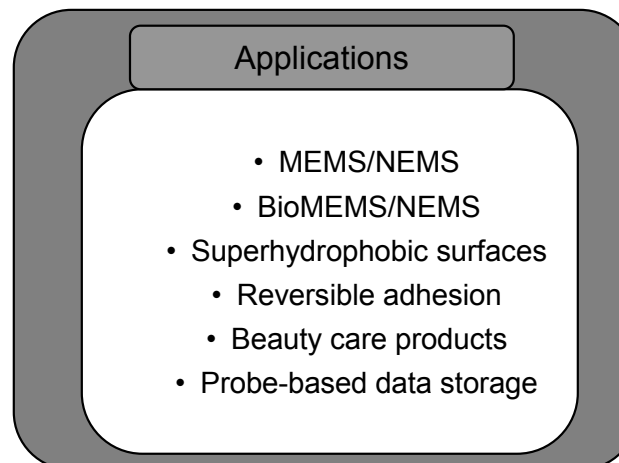




SWNT chemical sensor
(Kong et al., 2000)



MWNT ribbons
(Zhang et al., 2005)





Nanoprobe Laboratory for Bio- & Nanotechnology and Biomimetics



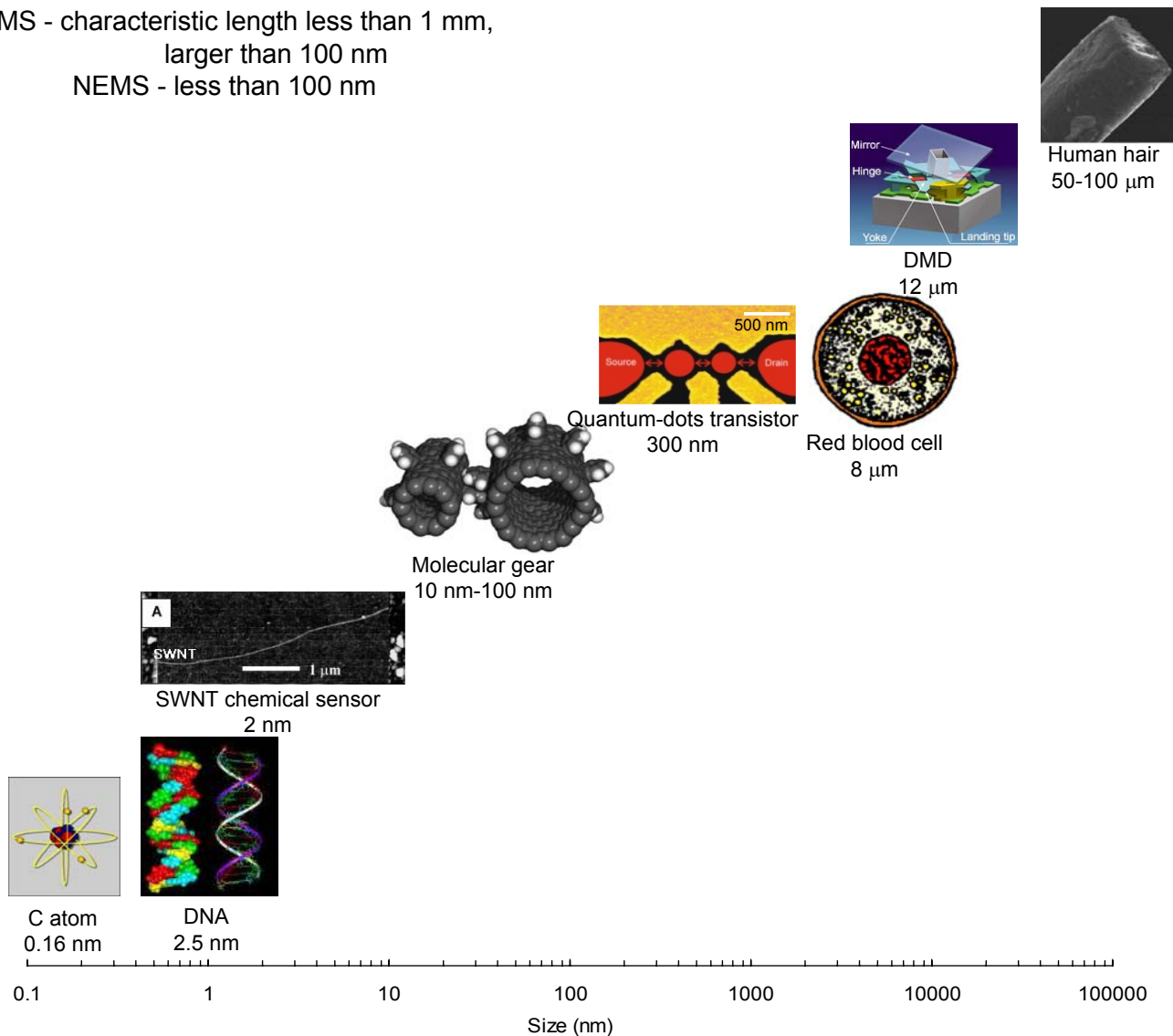
Outline

- Background
 - Definition of MEMS/NEMS and characteristic dimensions
 - Examples of MEMS/NEMS and BioMEMS/bioNEMS with tribology and mechanics issues
- Experimental
 - Atomic force/Friction force microscope (AFM/FFM)
- Tribological Studies of Lubricants
 - Perfluoropolyether lubricants and self-assembled monolayers
- Bioadhesion Studies
 - Surface modification approaches to improve bioadhesion
- Hierarchical Nanostructures for Superhydrophobicity and self cleaning (Lotus Effect)
 - Roughness optimization for superhydrophobic and self cleaning surfaces
 - Experimental studies
- Hierarchical Nanostructures for Reversible Adhesion (Gecko Feet)
 - Hierarchical structure for adhesion enhancement
 - Roughness optimization for reversible dry adhesives (*not included*)

Background

Definition of MEMS/NEMS and characteristic dimensions

MEMS - characteristic length less than 1 mm,
larger than 100 nm
NEMS - less than 100 nm



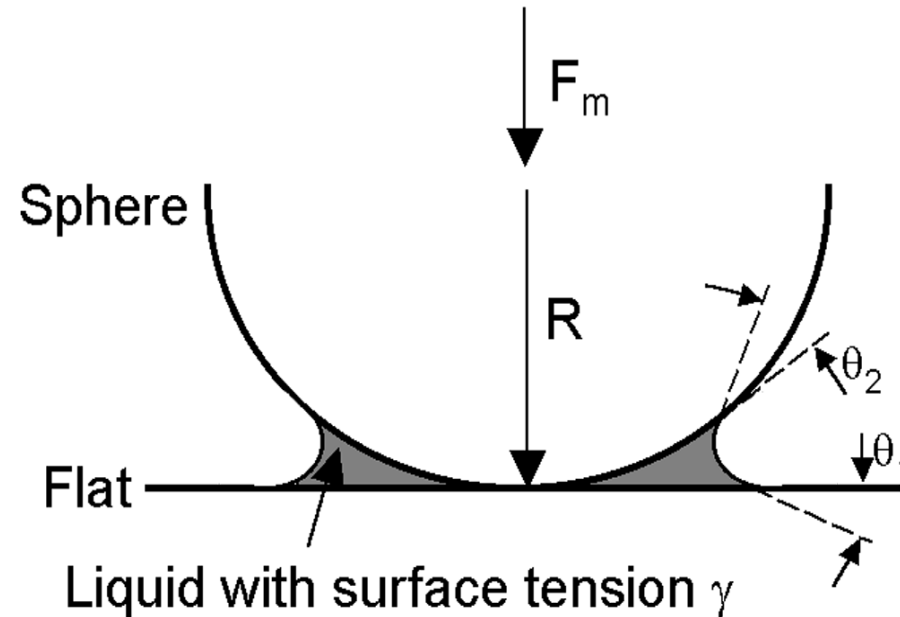
Characteristic dimensions in perspective

B. Bhushan, *Springer Handbook of Nanotechnology*, Springer, 2nd ed. (2007)

Nanoprobe Laboratory for Bio- & Nanotechnology and Biomimetics



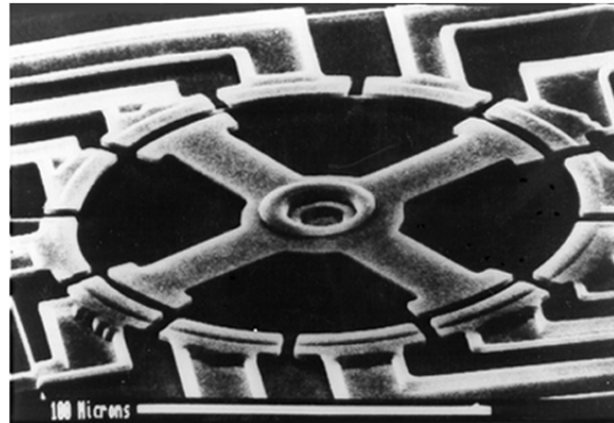
Stiction – High static friction force required to initiate sliding. Primary source is liquid mediated adhesion



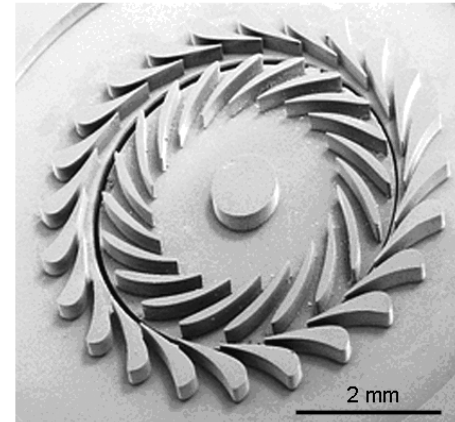
$$F_m = 2\pi R\gamma (\cos\theta_1 + \cos\theta_2)$$

Formation of meniscus and contribution to the attractive force

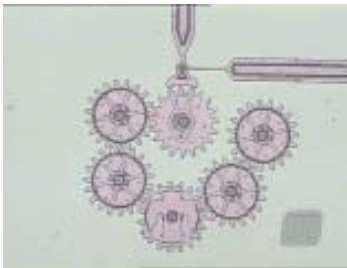
Examples of MEMS with tribology and mechanics issues



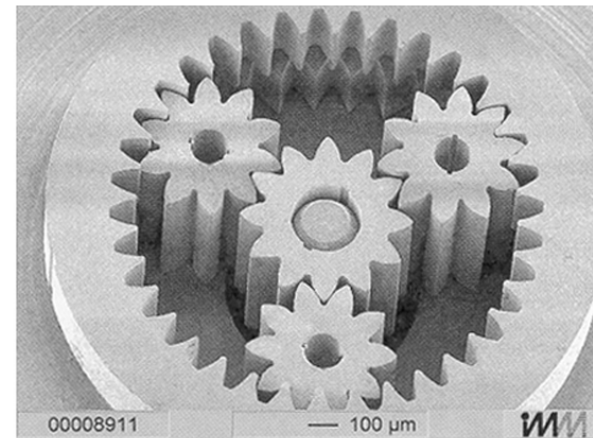
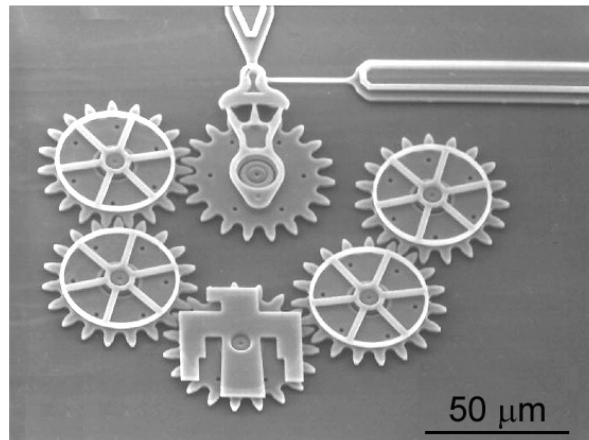
Electrostatic micromotor
(Tai et al., 1989)



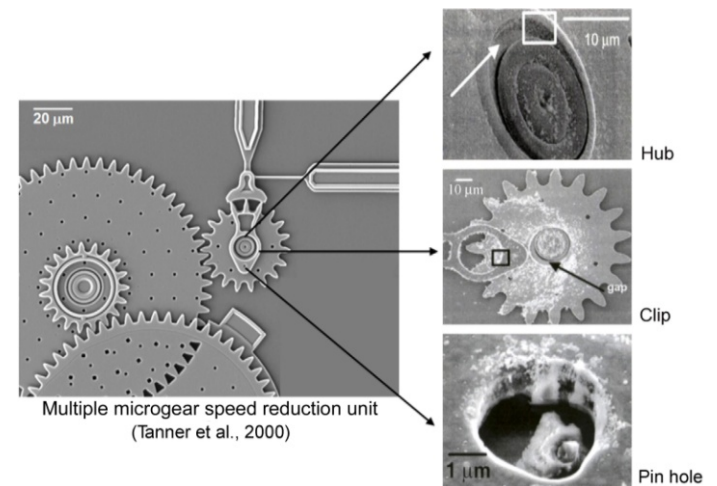
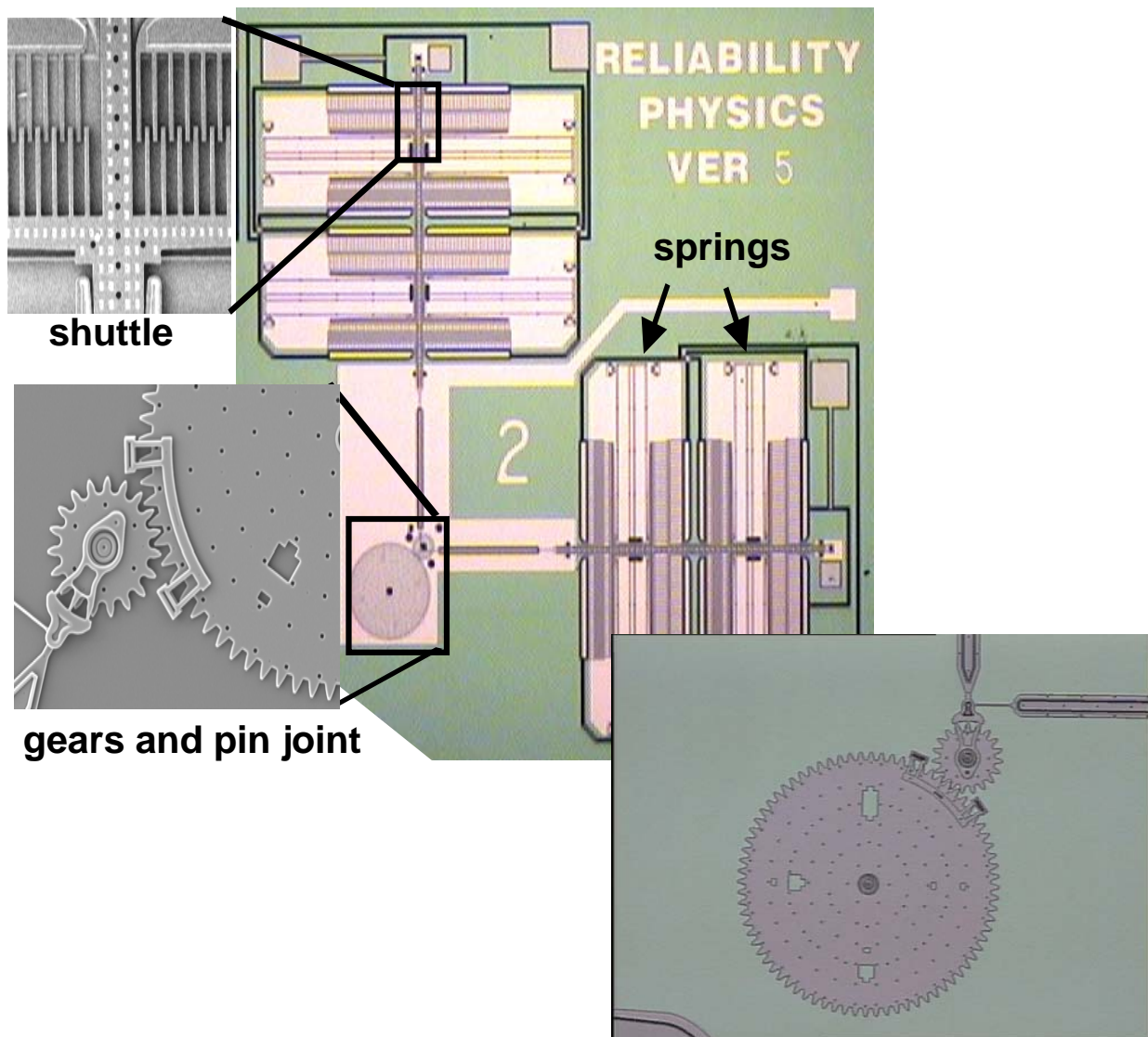
Microturbine bladed rotor and
nozzle guide vanes on the stator
(Spearing and Chen, 2001)



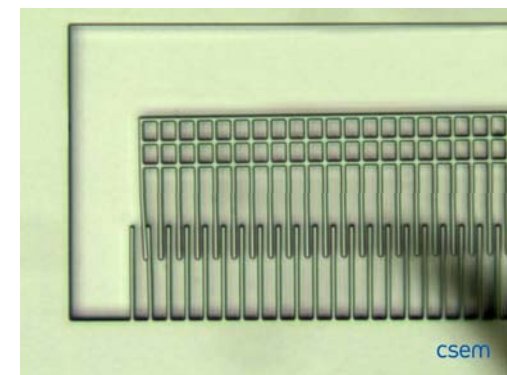
Six-gear chain
(www.sandia.gov)



Ni-Fe wolfram-type gear system
by LIGA (Lehr et al., 1996)



Microgear unit can be driven at speeds up to 250,000 RPM. Various sliding comp. are shown after wear test for 600k cycles at 1.8% RH (Tanner et al., 2000)

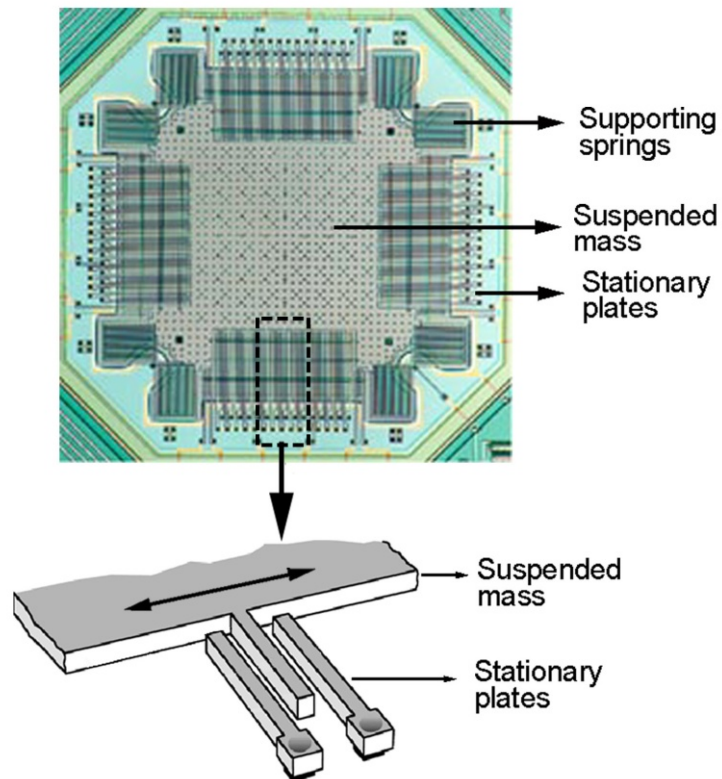


Microengine driven by electrostatically-actuated comb drive

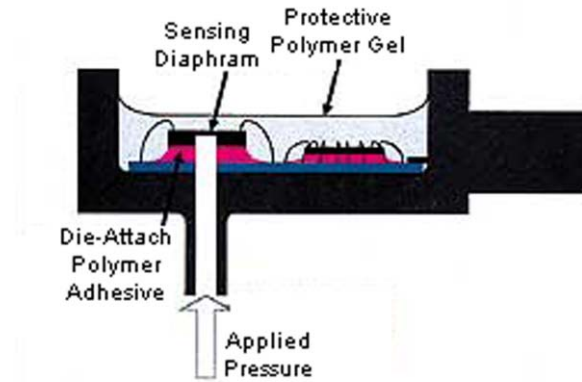
Sandia Summit Technologies (www.mems.sandia.gov)

Stuck comb drive

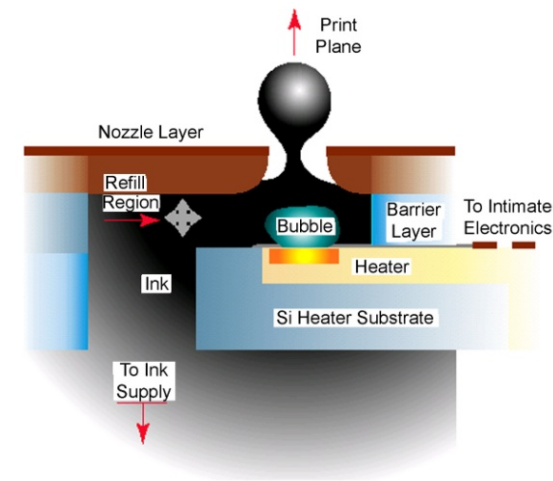
Examples of commercial MEMS devices



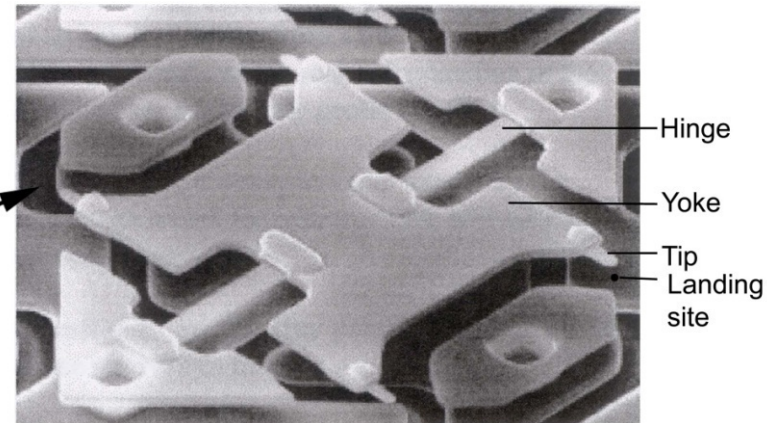
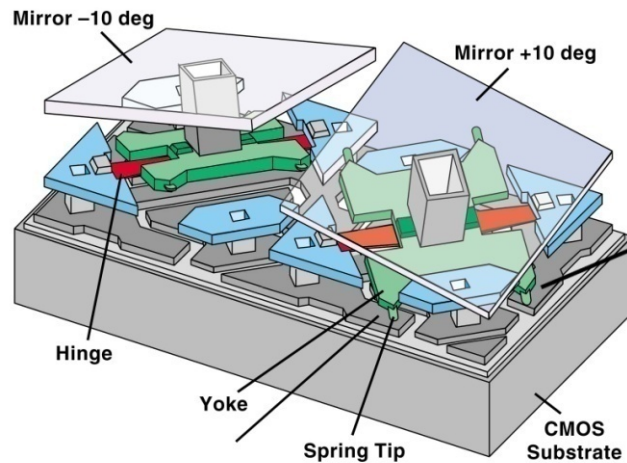
Capacitive type silicon accelerometer for automotive sensory applications (Sulouff, 1998)



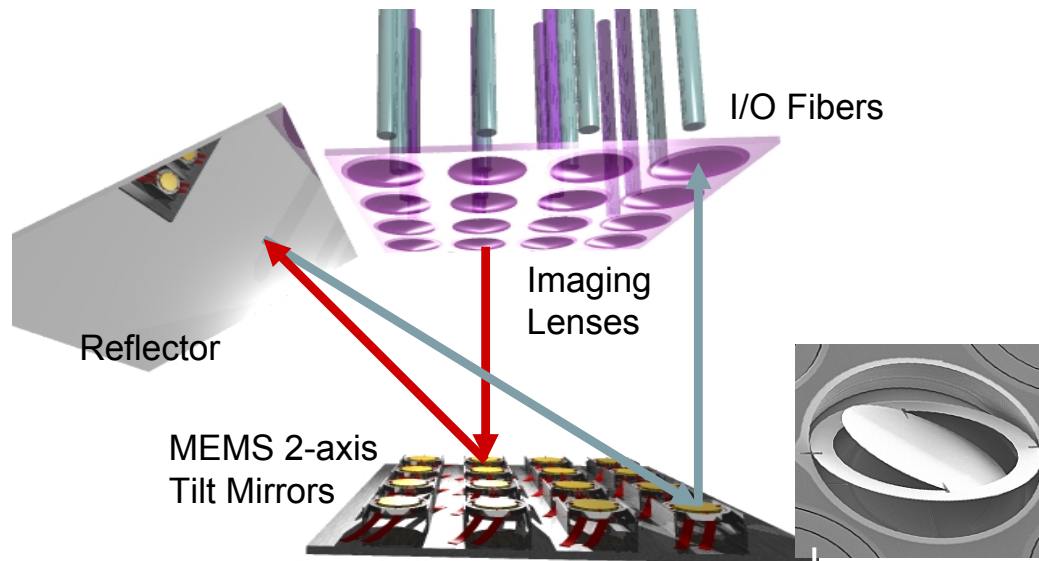
Piezoresistive type pressure sensor (Parsons, 2001)



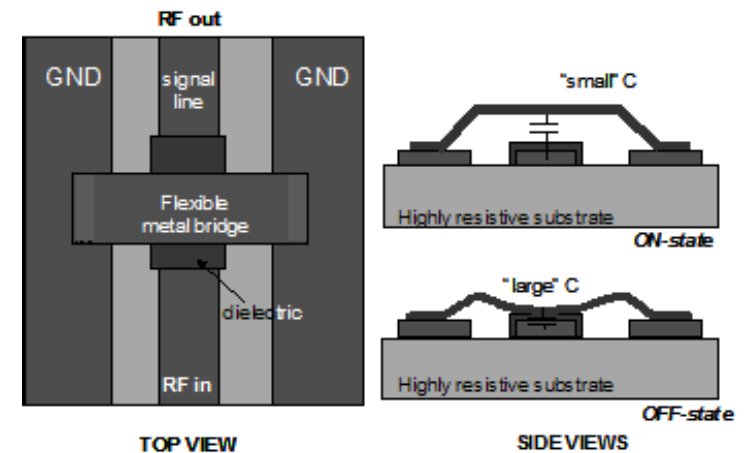
Thermal inkjet printhead (Baydo and Grosup, 2001)



Digital micromirror device for displays (Hornbeck, 1999)

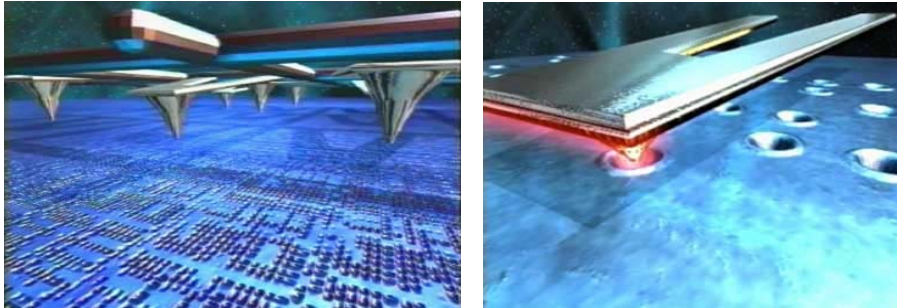


Tilt mirror arrays for switching optical signal in input and output fiber arrays in optical crossconnect for telecom.
(Aksyuk et al., 2003)



RF microswitch
(Courtesy IMEC, Belgium)

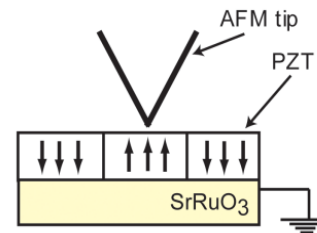
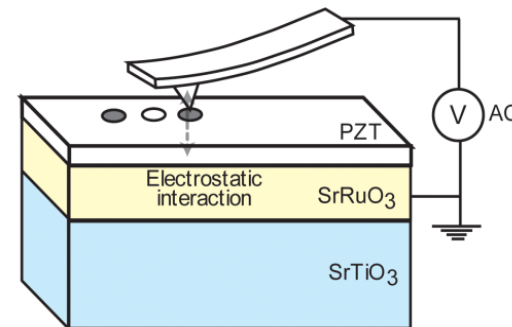
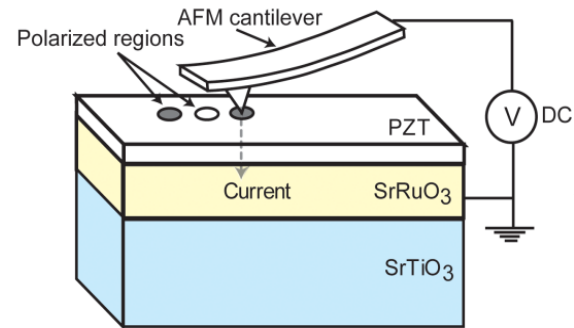
Examples of NEMS



32 x 32 tip array
(<http://www.ibm.com>)

Probe-based NEMS data storage
based on thermomechanical recording

- Integrated tip heaters consist of tips of nanoscale dimension.
- Thermomechanical recording is performed on an about 40-nm thick polymer medium on Si substrate.
- Heated tip to about 400 °C contacts with the medium for recording.
- Wear of the heated tip is an issue.

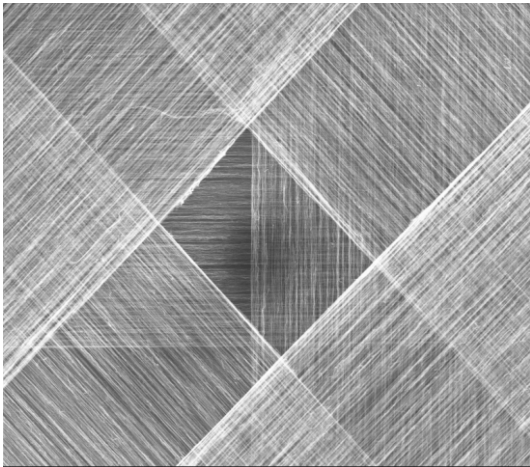


Probe-based NEMS data storage based on
ferroelectric recording

- Ferroelectric material, typically lead zirconate titanate (PZT)
- Electrical current switches between two different polarization states by applying short voltage pulses (~10 V, ~100 ms), resulting in recording. Temperature rise on the order of 80°C is expected.
- Piezoresponse force can be read out by applying an AC voltage of 1 V.
- Wear of the tip and medium at 80°C is an issue.
- Furthermore, the tip does not need to be in contact with medium during readback.

CNT-based Nanostructures

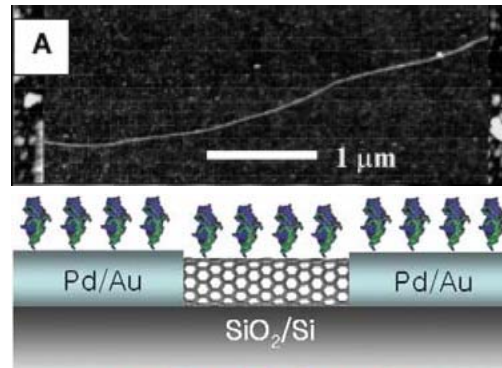
MWNT Sheet



(Zhang et al., 2005)

Mechanical properties of nanotube ribbons, such as the elastic modulus and tensile strength, critically rely on the adhesion and friction between nanotubes.

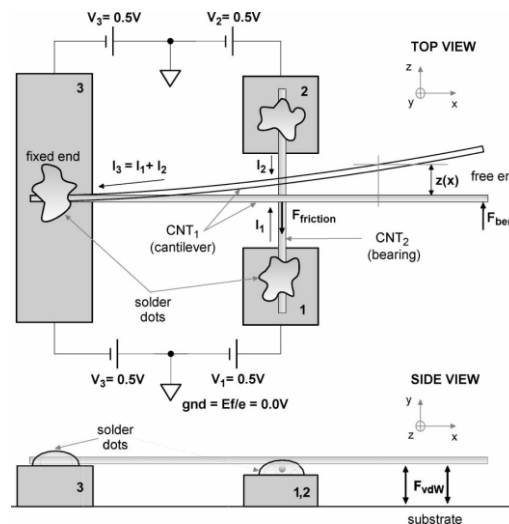
SWNT biosensor



(Chen et al., 2004)

The electrical resistance of the system is sensitive to the adsorption of molecules to the nanotube/electrode. Adhesion should be strong between adsorbents and SWNT.

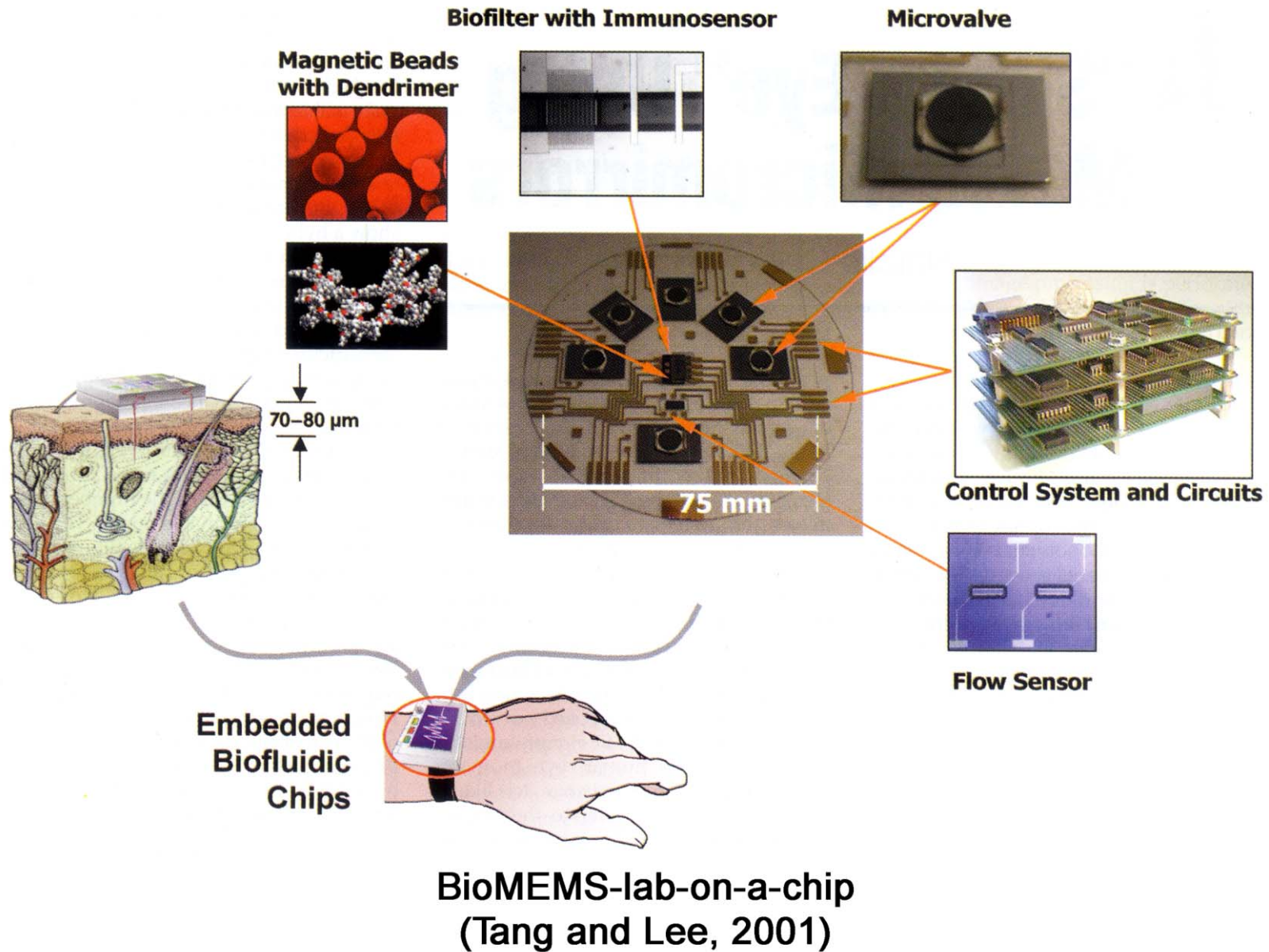
Nanotube bioforce sensor

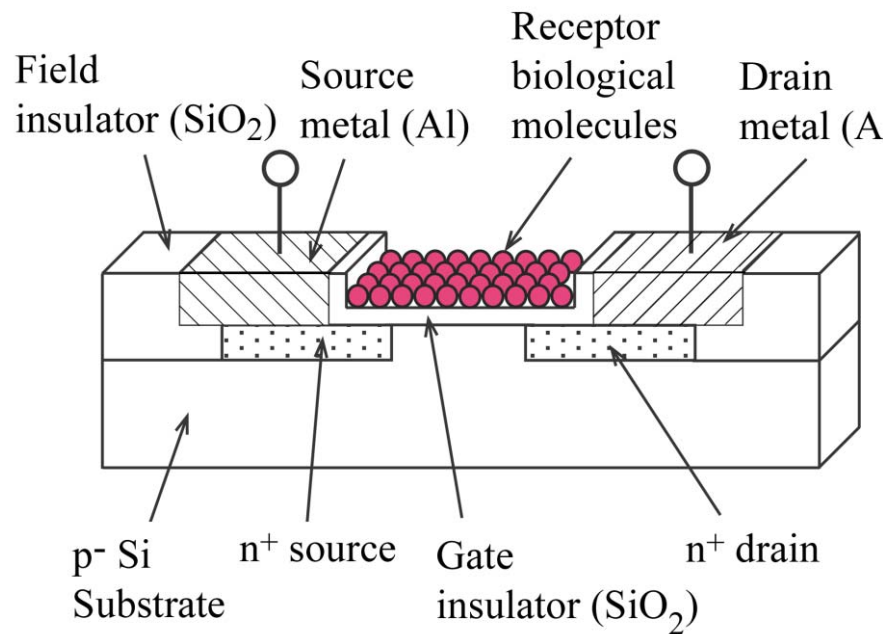


(Roman et al., 2005)

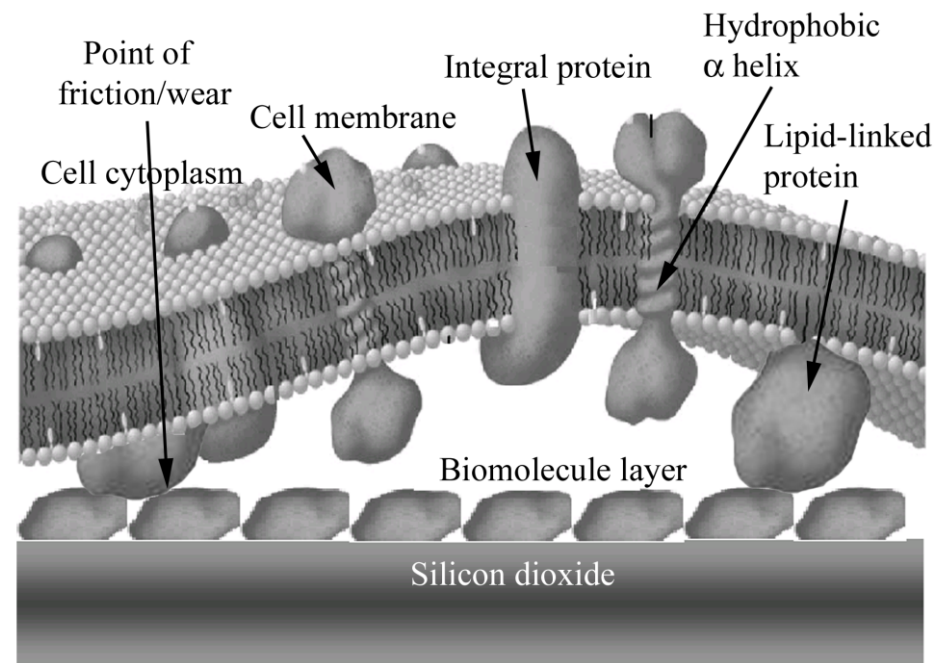
Force applied at the free end of nanotube cantilever is detected as the imbalance of current flowing through the nanotube bearing supporting the nanotube cantilever. The deflection of nanotube cantilever involves inter-tube friction.

Examples of BioMEMS/BioNEMS

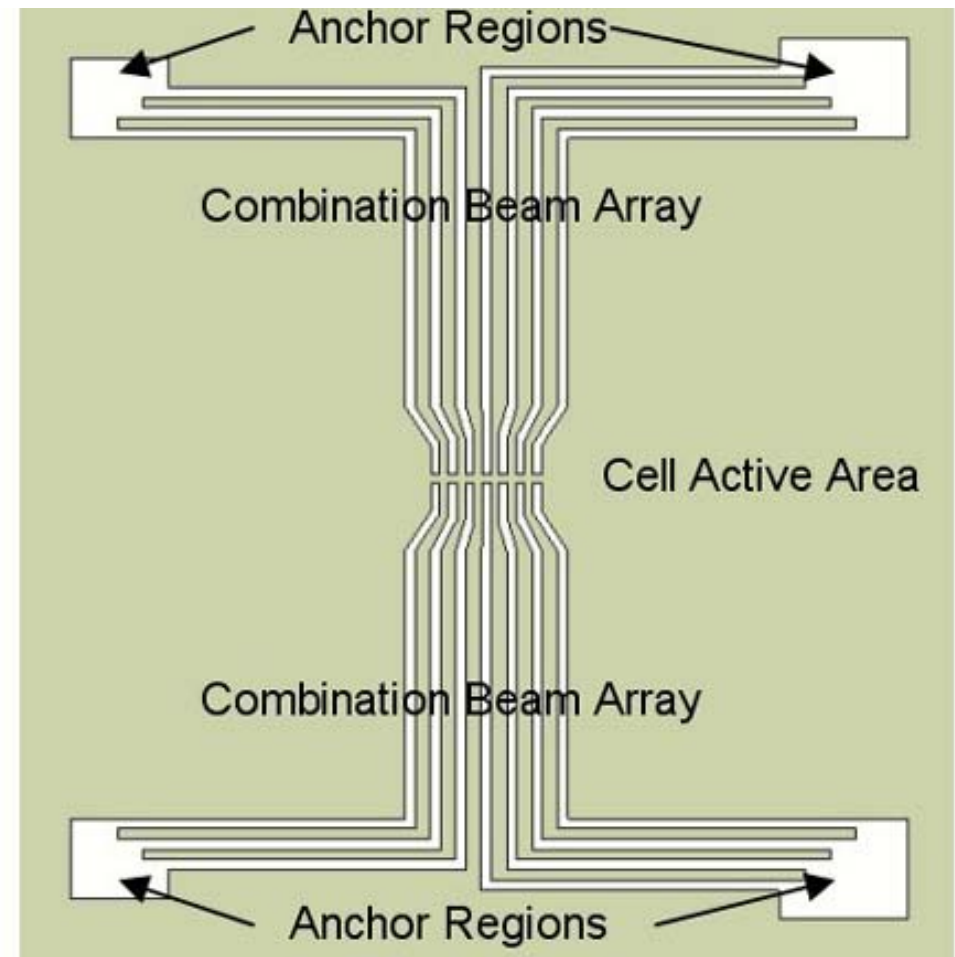
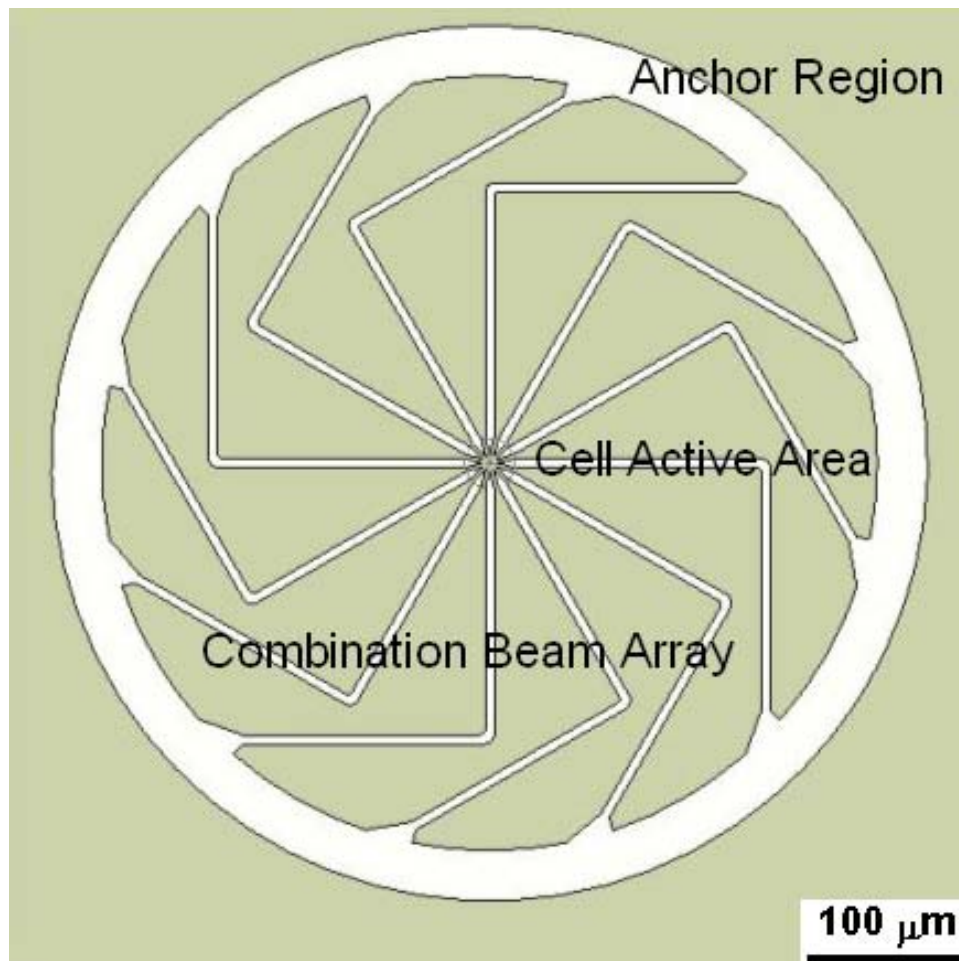




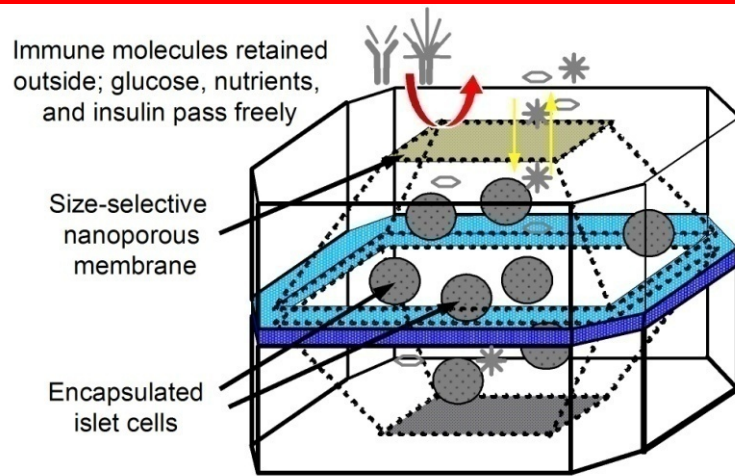
BioFET sensor
(Bhushan, Lee et al., 2005)



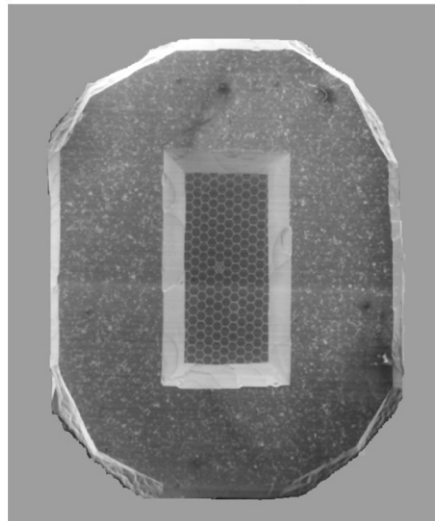
The generating points of friction and wear due to interaction of a biomolecular layer on a synthetic microdevice with tissue
(Bhushan et al., 2006)



Two examples of polymer MEMS designed to measure cellular forces
(Wei, Bhushan, Hansford and Ferrell, 2005)

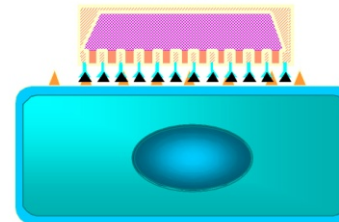


One half of biocapsule

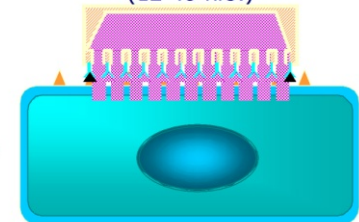


Implantable immunoisolation biocapsule
(Hansford et al., 2001)

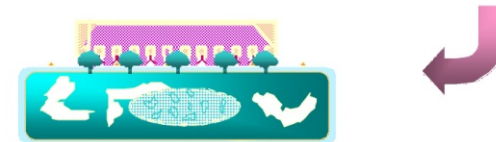
1. Binding (0-8 hours after injection)



2. Plug rupture, drug Release (12-48 hrs.)

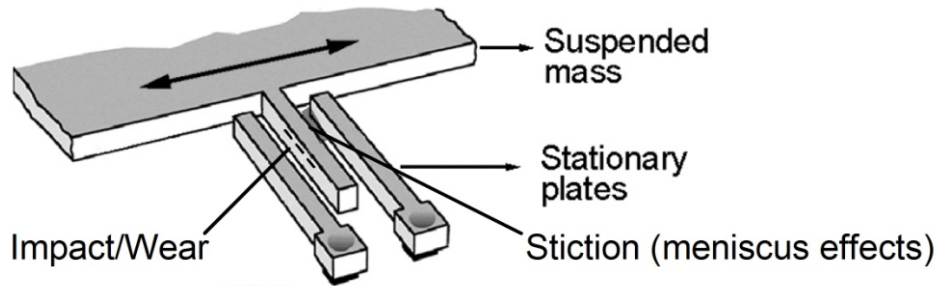


3. Pore Formation - cell lysis and death (12-48 hrs)

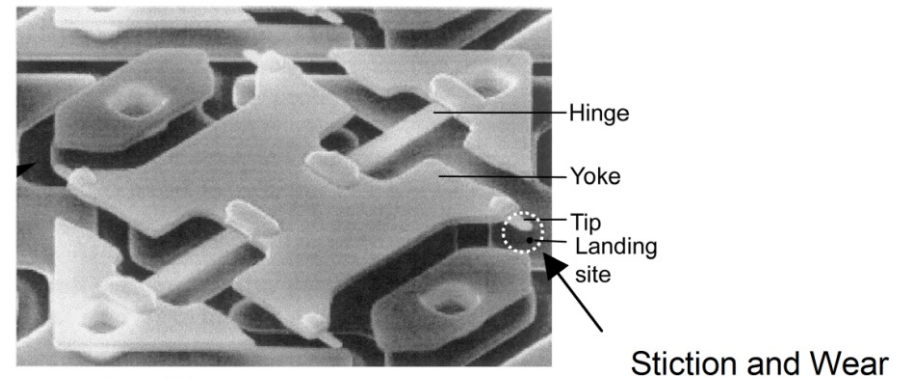


Intravascular nanoparticles for search
and destroy diseased blood cells
(Martin and Grove, 2001)

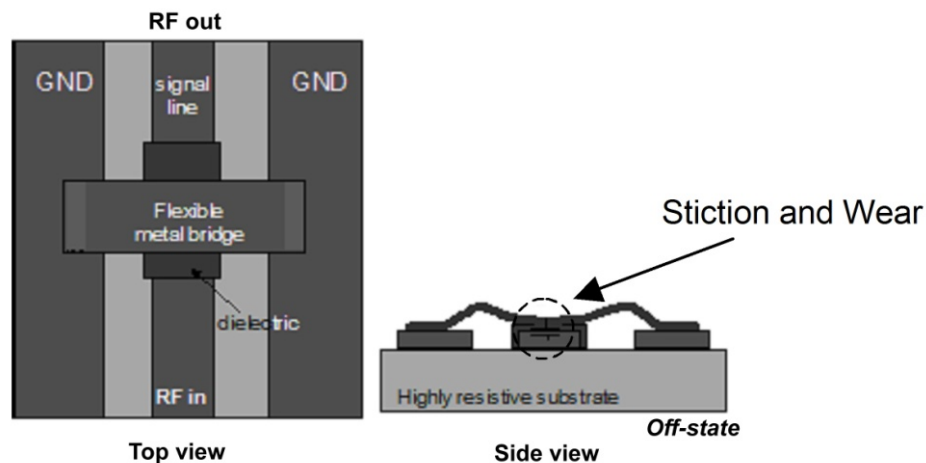
Tribology and mechanics issues during device operation



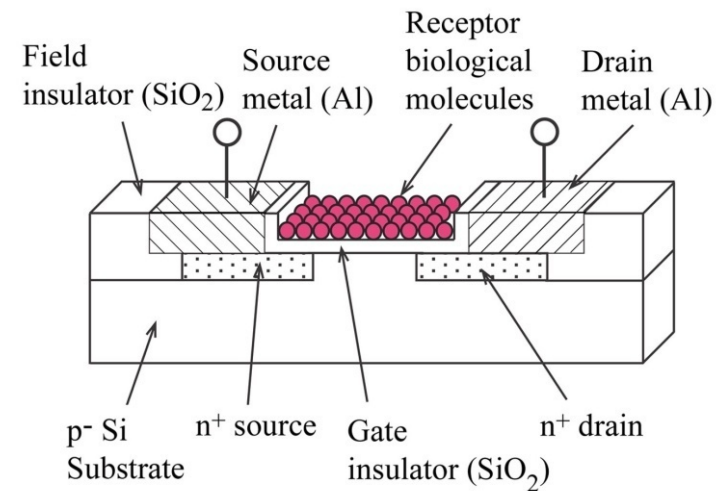
Capacitive type accelerometer



Digital micromirror device



RF Microswitch



BioFET sensor

Need to address tribology and mechanics issues

- The tribology and mechanics problems can drastically compromise device performance and reliability. To solve these problems, there is a need to **develop a fundamental understanding** of adhesion, friction/stiction, wear and the role of surface contamination and environment in MEMS/NEMS and BioMEMS/NEMS. This can be done by studying
 - ❑ Tribology and mechanics of MEMS/NEMS materials
 - ❑ Lubricant methods for MEMS/NEMS
 - ❑ Bioadhesion Studies
 - ❑ Development of superhydrophobic surfaces
 - ❑ Device level studies

Approach

- Use an AFM/FFM for imaging and to study adhesion, friction, scratch and wear properties of materials and lubricants, which better simulates MEMS/NEMS and BioMEMS/BioNEMS contacts
- Develop and employ techniques to measure tribological phenomena in devices

B. Bhushan et al., *Nature* **374**, 607 (1995); B. Bhushan, *Handbook of Micro/Nanotribology*, second ed., CRC Press, 1999;
B. Bhushan, *Introduction to Tribology*, Wiley, NY, 2002; B. Bhushan, *Springer Handbook of Nanotechnology*, 2nd ed., 2007;
B. Bhushan, *Nanotribology and Nanomechanics – An Introduction*, Springer, 2005.



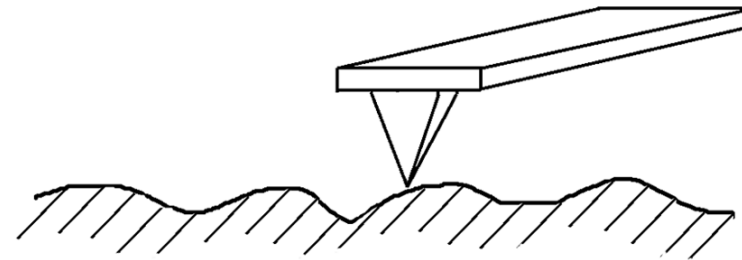
Experimental

Atomic force/Friction force microscope (AFM/FFM)

- At most interfaces of technological relevance, contact occurs at numerous asperities. It is of importance to investigate a single asperity contact in the fundamental tribological studies.

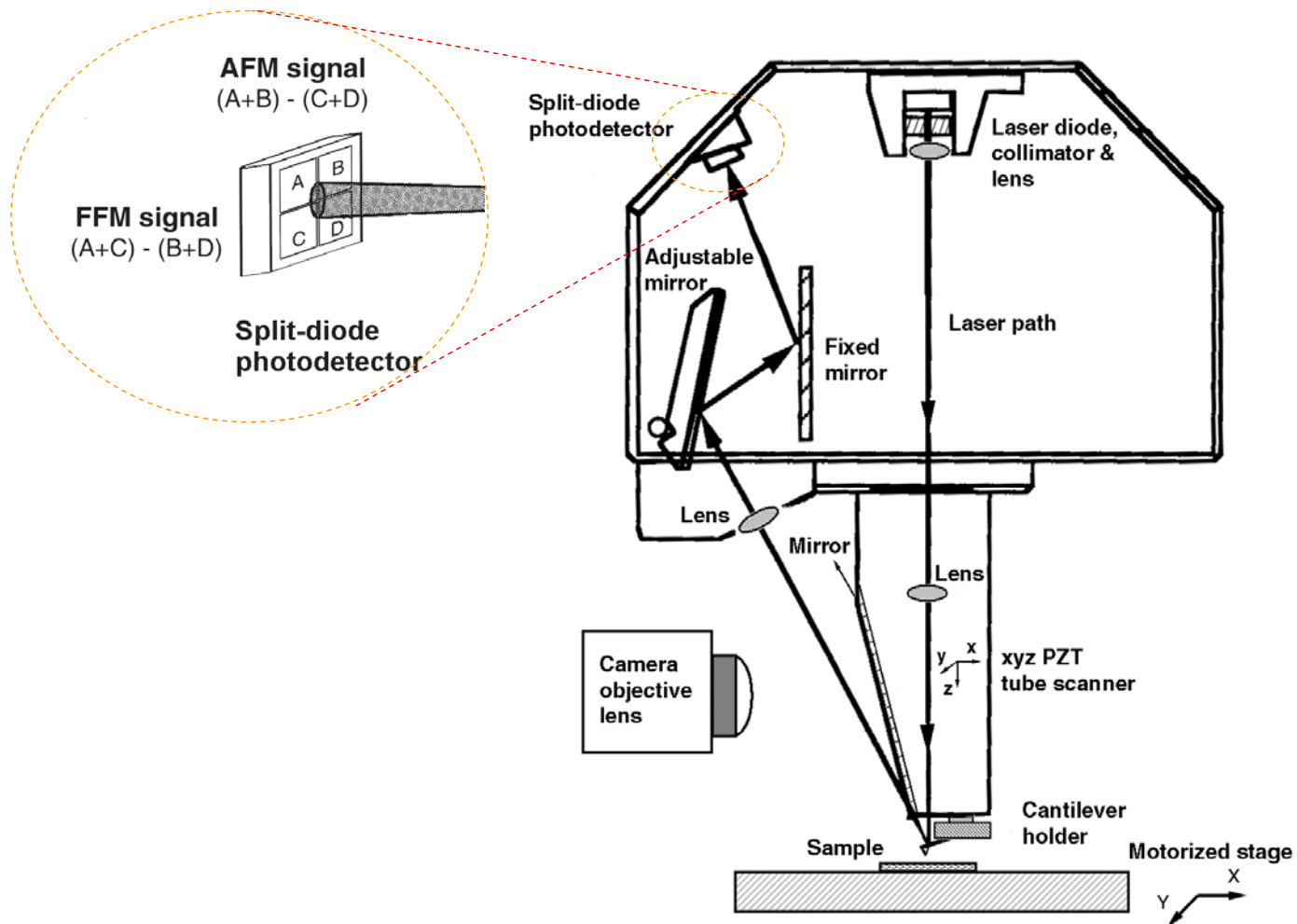


Engineering Interface

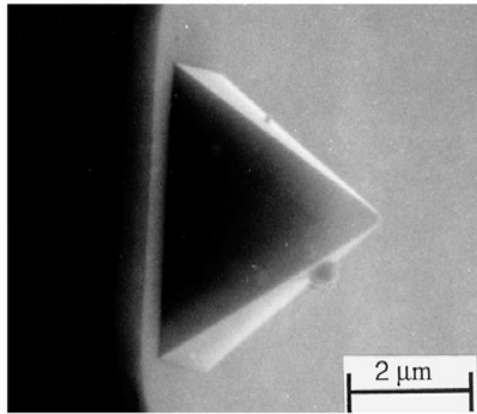


Tip - based microscope allows simulation of a single asperity contact

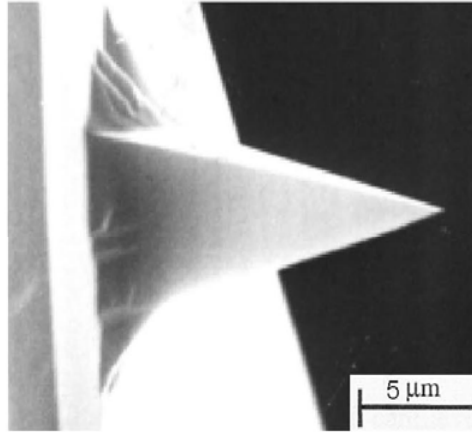
- Nanotribological studies are needed
 - To develop fundamental understanding of interfacial phenomena on a *small* scale
 - To study interfacial phenomena in *micro-* or *nanostructures* and performance of ultra-thin films used in MEMS/NEMS components



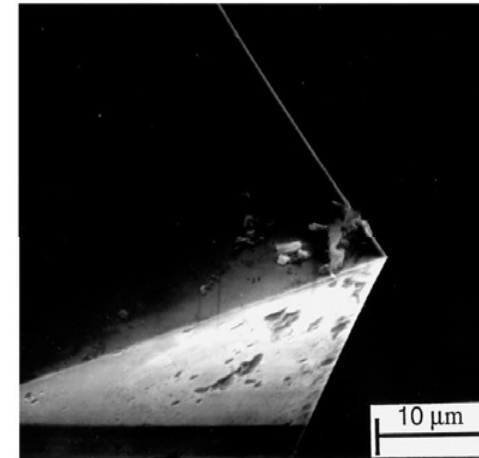
Large sample AFM/FFM



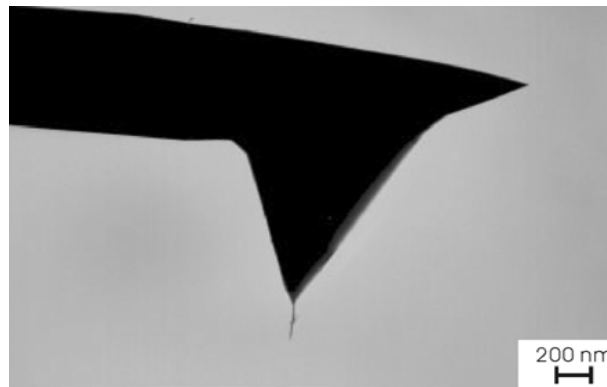
Square pyramidal
silicon nitride tip



Square pyramidal
Single-crystal silicon tip



Three-sided pyramidal
(natural) diamond tip



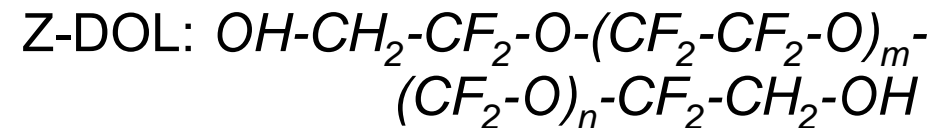
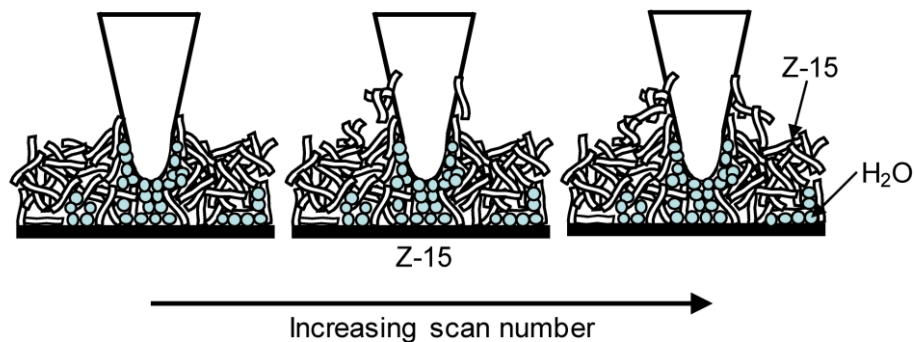
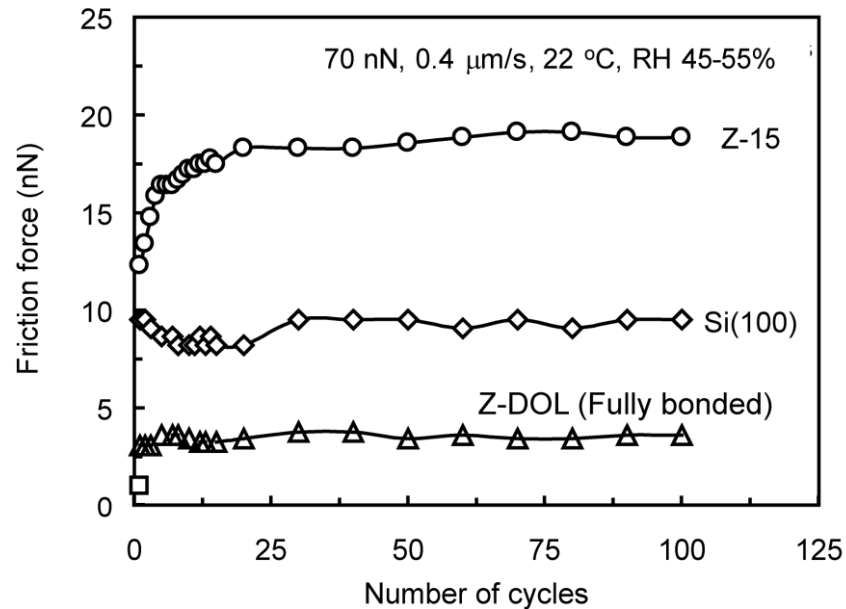
Carbon nanotube tip

Various AFM tips

Tribological Studies of Lubricants

- **Chemically bonded liquid and solid lubricants with monolayer thicknesses are desired for low friction and wear.**
- **Lubricants must be hydrophobic to minimize effect of environment.**
 - **Perfluoropolyether (PFPE) lubricants**
 - **Self-assembled monolayers (SAMs)**

Perfluoropolyether lubricants



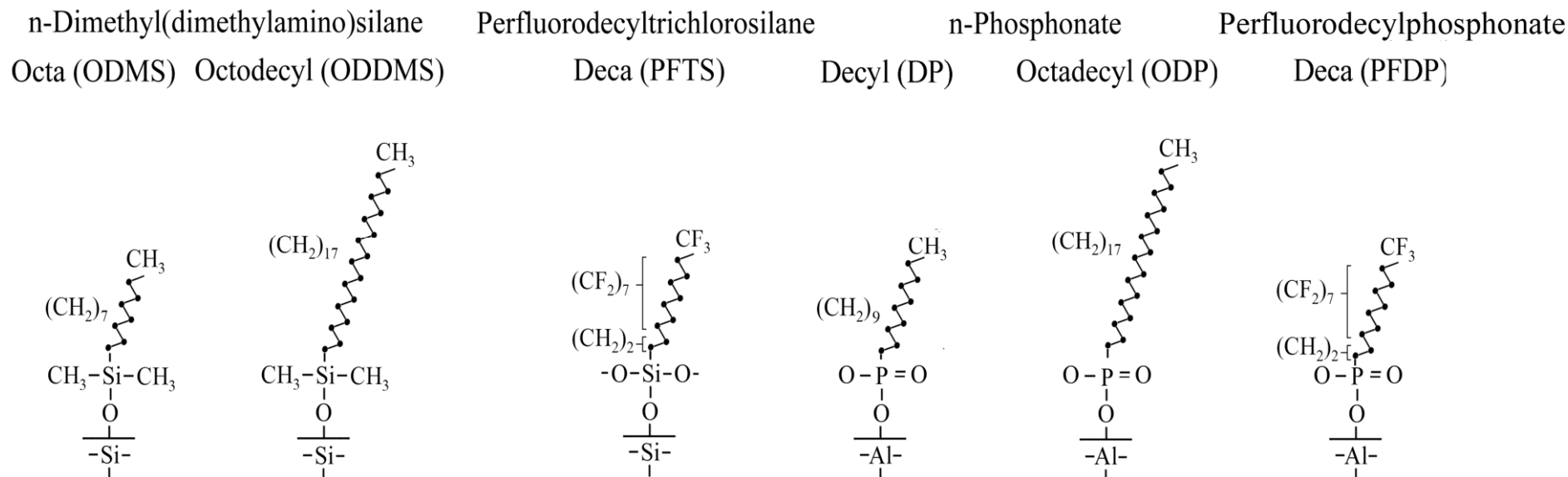
- During cycling tests, the friction Z-DOL (BW) exhibits the lowest friction and Z-15 shows negative effect.
- During cycling tests, the friction of Si(100) and Z-DOL (BW) does not change. The friction of Z-15 film initially increases and reaches to a higher and stable value. The initial rise occurs because of the molecular interaction between the attached Z-15 molecules to the tip and the Z-15 molecules on the film surface.

Durability data

V. N. Koinkar and B. Bhushan, *J. Appl. Phys.* **79**, 8071 (1996); *J. Vac. Sci. Technol. A*, **14**, 2378 (1996);

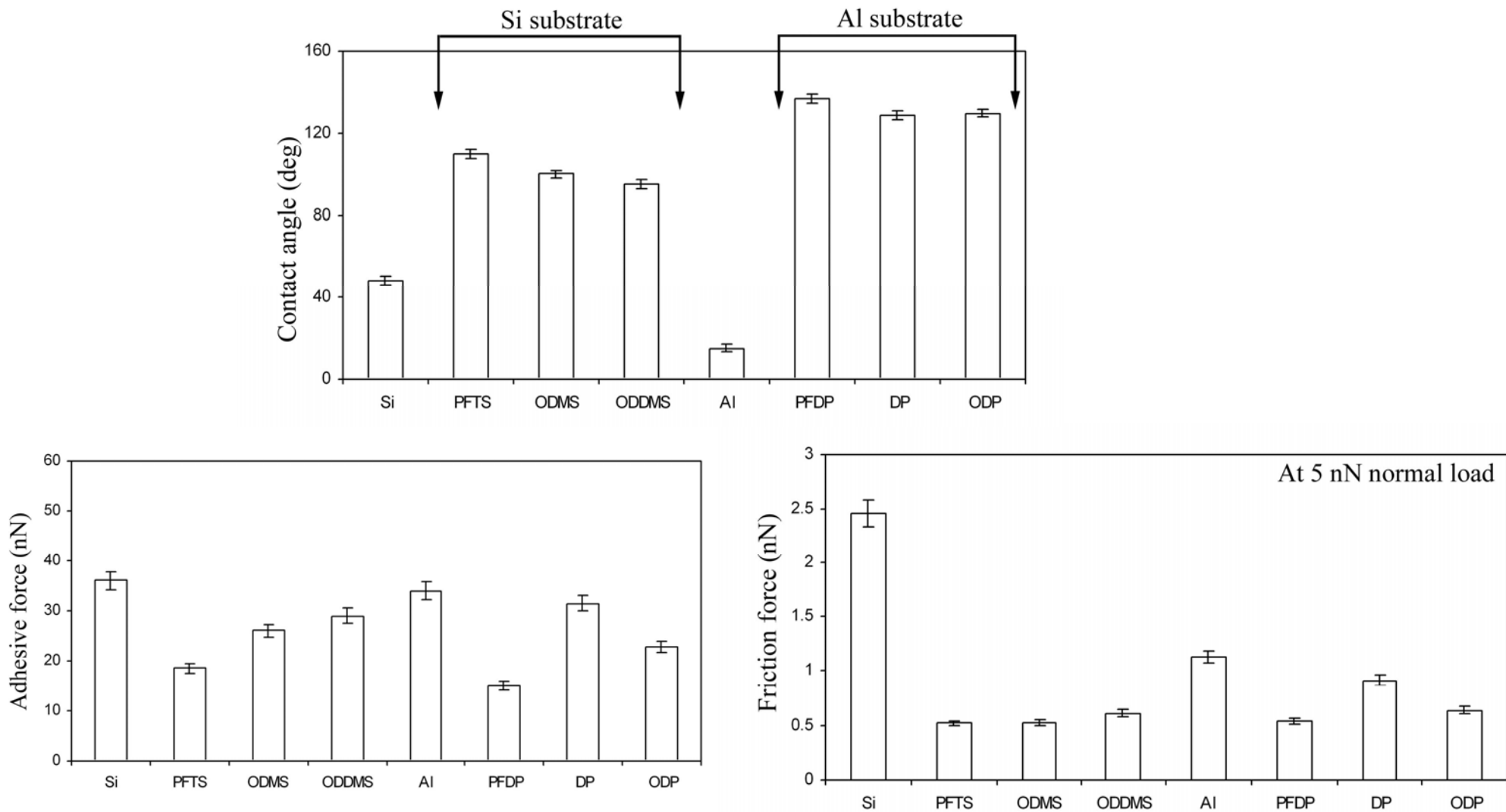
H. Liu and B. Bhushan, *Ultramicroscopy* **97**, 321 (2003)

Self-assembled monolayers (SAMs)



Perfluoroalkylsilane and alkylsilane SAMs were deposited on Si(111) with natural oxide and perfluoroalkylphosphonate and alkylphosphonate on Al.

B. Bhushan et al., *Langmuir*, **11**, 3189 (1995); H. Liu, B. Bhushan, W. Eck and V. Stadler, *J. Vac. Sci. Technol. A* **19**, 1234 (2001); B. Bhushan and H. Liu, *Phys. Rev. B* **63**, 255412 (2001); B. Bhushan et al., *Ultramicroscopy* **105**, 176 (2005); T. Kasai, B. Bhushan et al., *J. Vac. Sci. Technol. B* **23**, 905 (2005); N. S. Tambe and B. Bhushan, *Nanotechnology* **16**, 1549 (2005); Z. Tao and B. Bhushan, *Langmuir* **21**, 2391 (2005); B. Bhushan et al., *Microsyst. Technol.* **12**, 588 (2006); B. Bhushan and M. Cichomski, *J. Vac. Sci. Technol. A* **25**, 1285 (2007); E. Hoque et al., *J. Chem. Phys.* **124**, 174710 (2006); *J. Phys. Chem. B* **110**, 10855 (2006); *J. Phys. Chem. C* **111**, 3956 (2007); *J. Chem. Phys.* **126**, 114706 (2007); DeRose et al., submitted.

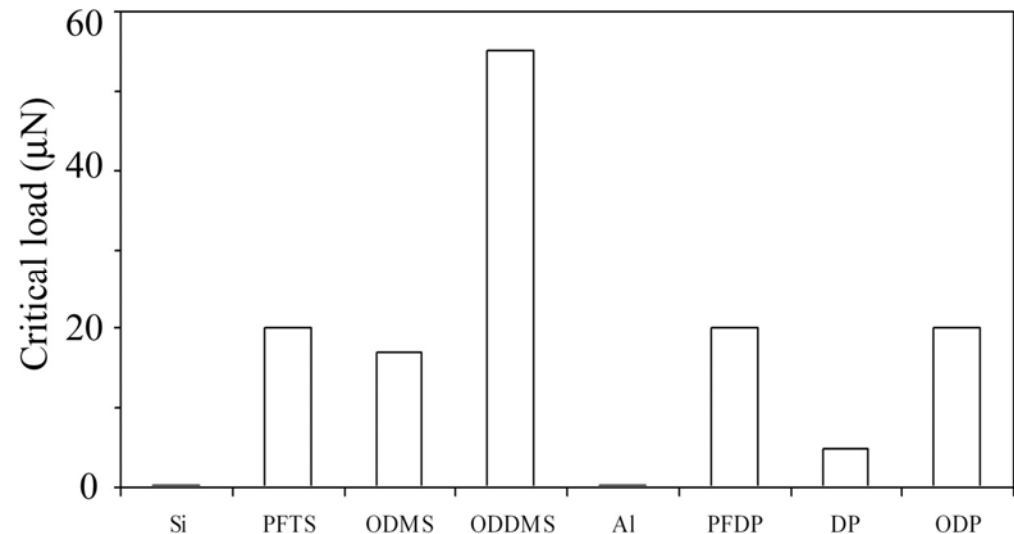
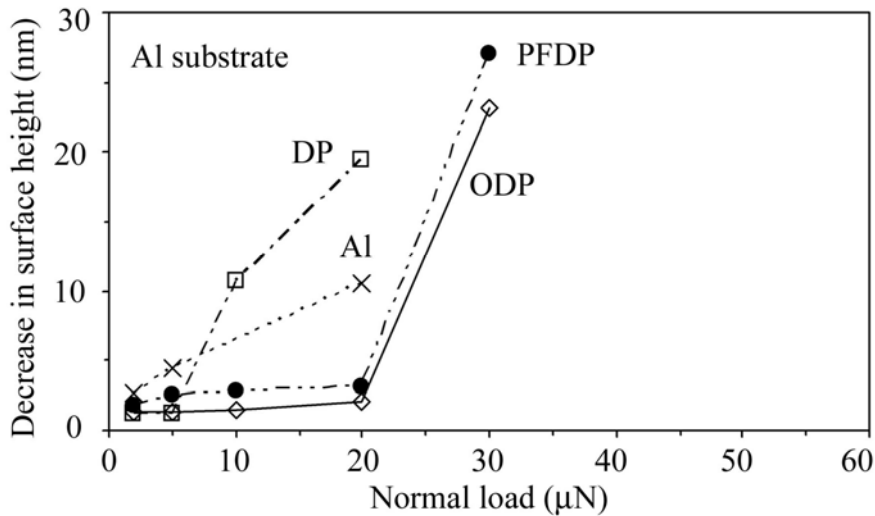
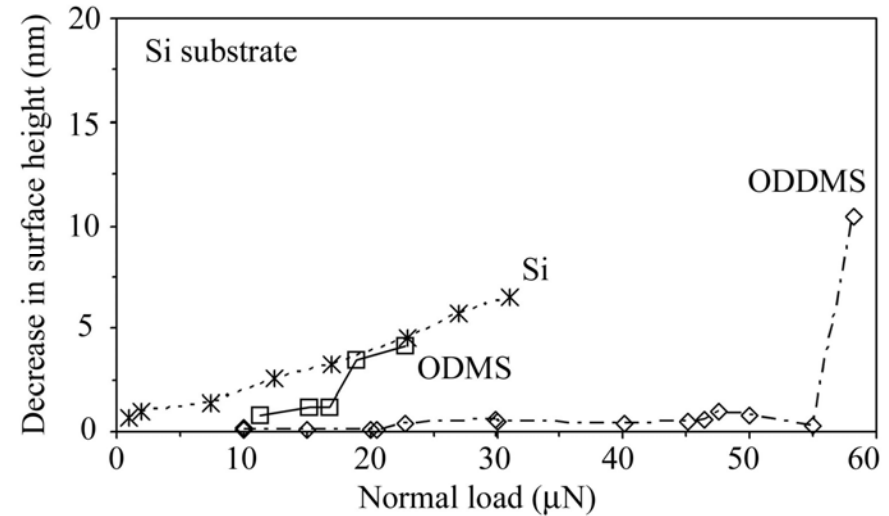
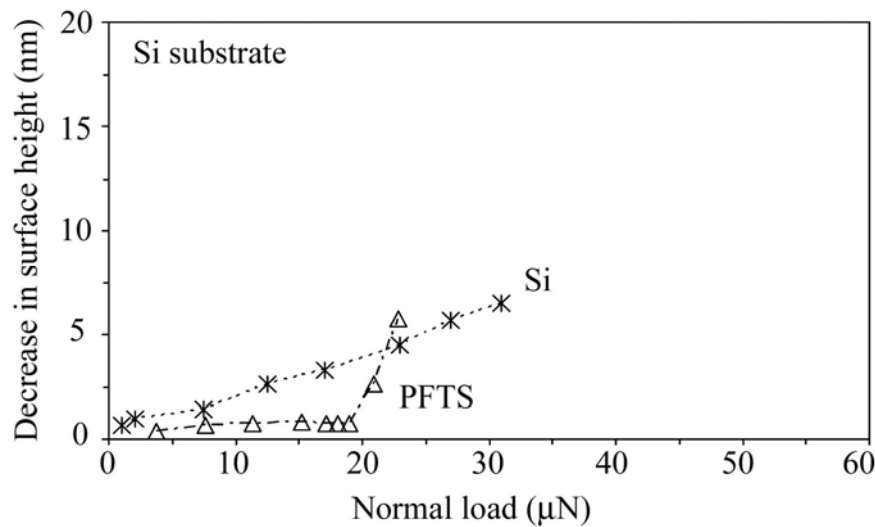


PFTS showed lower adhesive force than and comparable coefficient of friction to ODMS and ODDMS.

Chain length has little effect.

DP and ODP showed higher coefficient of friction and comparable adhesive force to ODMS and ODDMS.

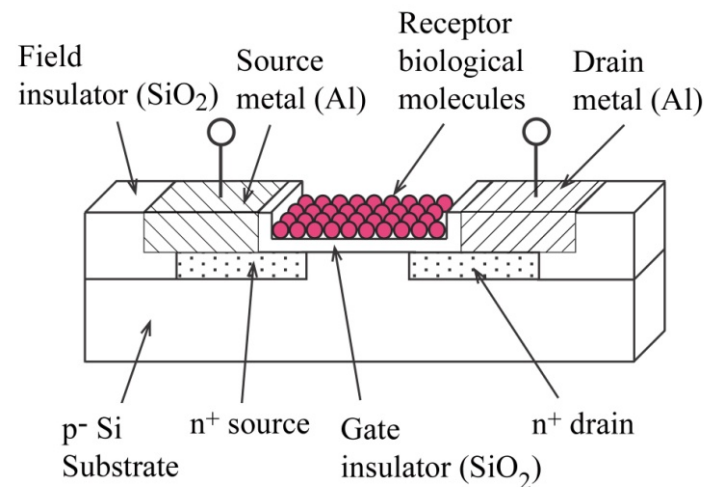
AFM Microwear



A critical normal load was observed for SAMs, higher than that for substrates. Critical loads are lowest for ODMS and DP, moderate for PFTS, PFTP and ODP, and highest for ODDMS.

Bioadhesion Studies

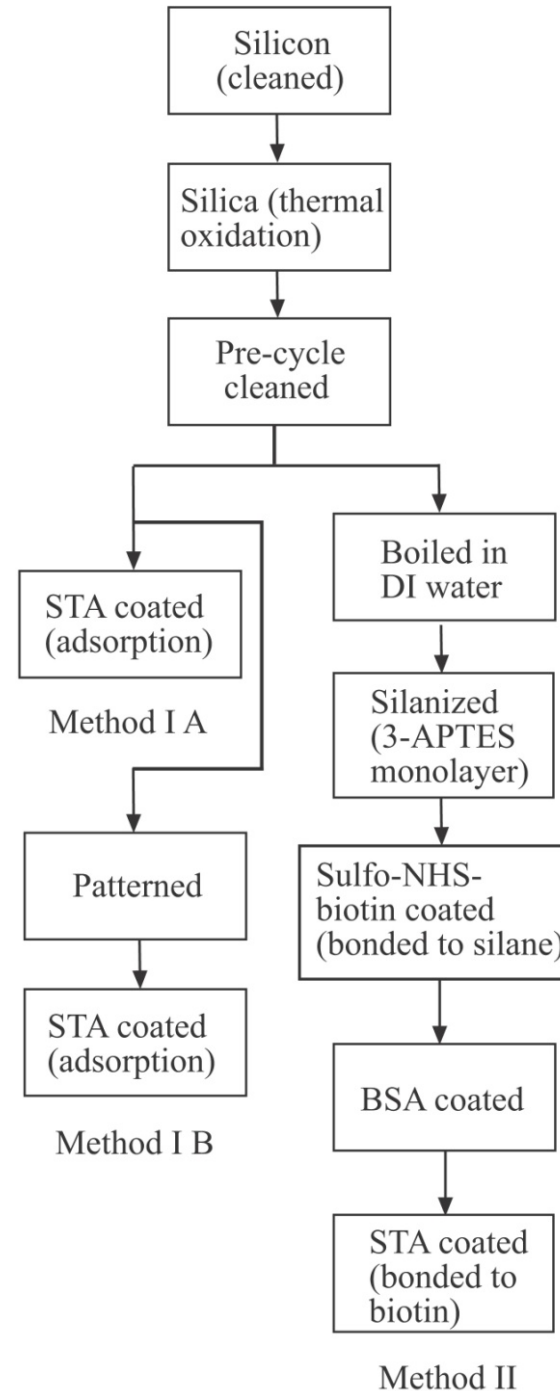
- Study surface modification approaches - nanopatterning and chemical linker method to improve adhesion of biomolecules on silicon based surfaces.



BioFET sensor
(Bhushan et al., 2005)

B. Bhushan et al., *Acta Biomaterialia* **1**, 327 (2005) ; *ibid* **2**, 39 (2006); Lee et al., *J. Vac. Sci. Technol. B* **23**, 1856 (2005) ; Tokachichu and Bhushan, *IEEE Trans. Nanotech.* **5**, 228 (2006); Eteshola et al., *J. Royal Soc. Interf.* **5**, 123 (2008)

Sample preparation

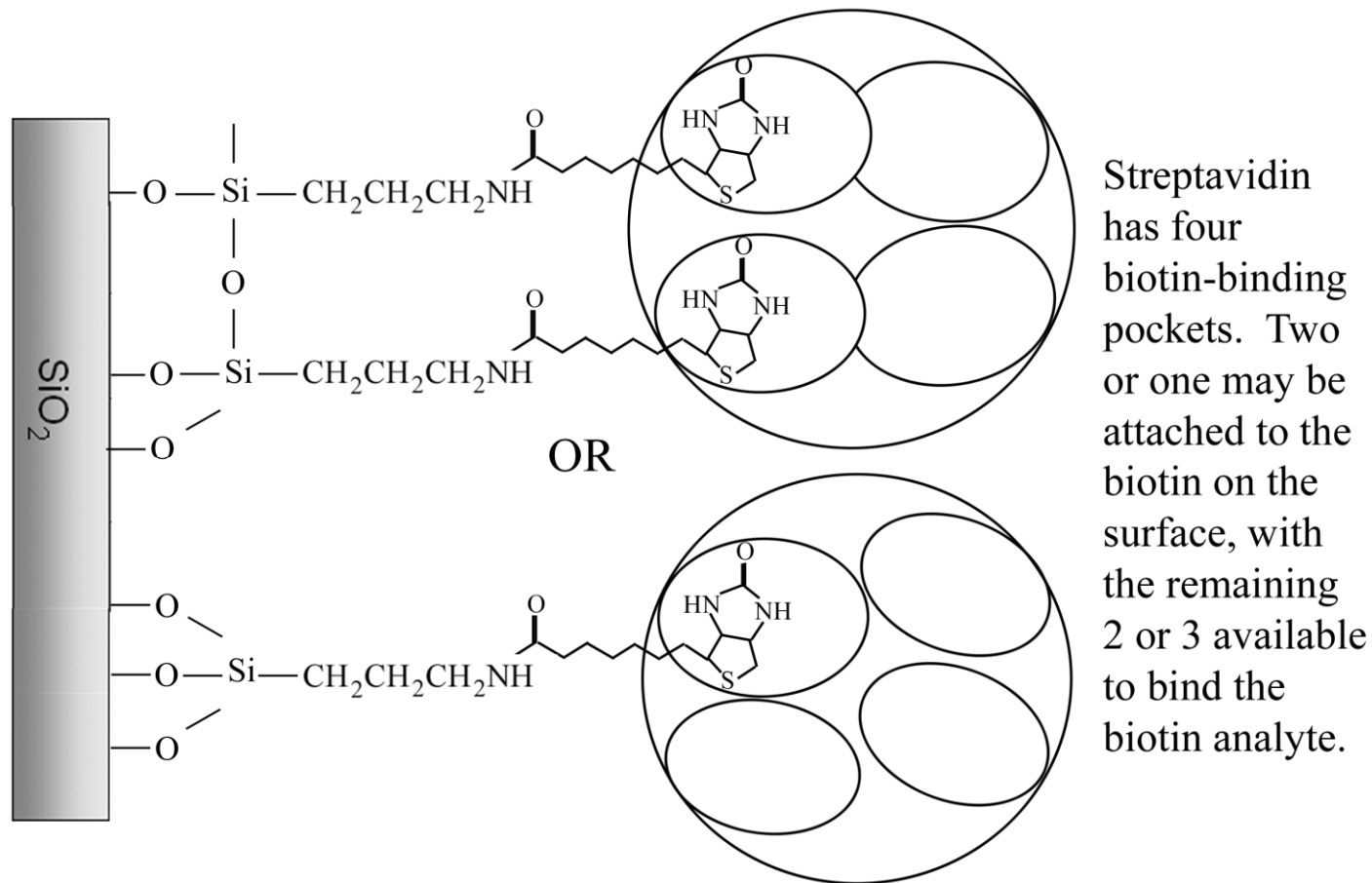


STA: Streptavidin

APTES: Aminopropyltriethoxysilane

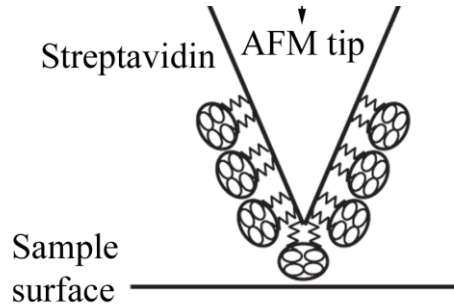
NHS: N-hydroxysuccinimido

BSA: Bovine serum albumin

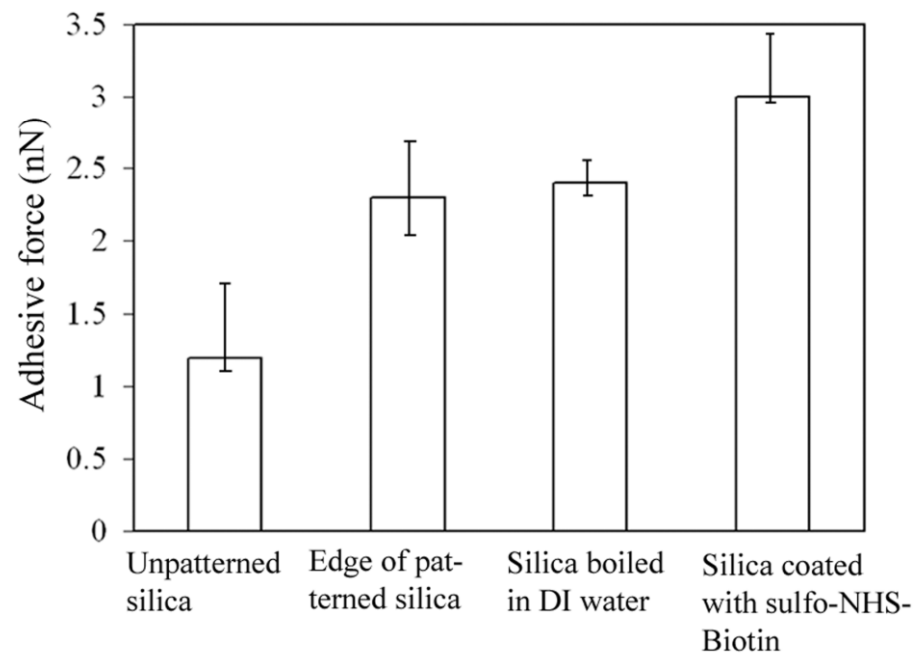


Schematic representation of deposition of streptavidin (STA) by chemical linker method

Adhesion measurements in PBS with functionalized tips

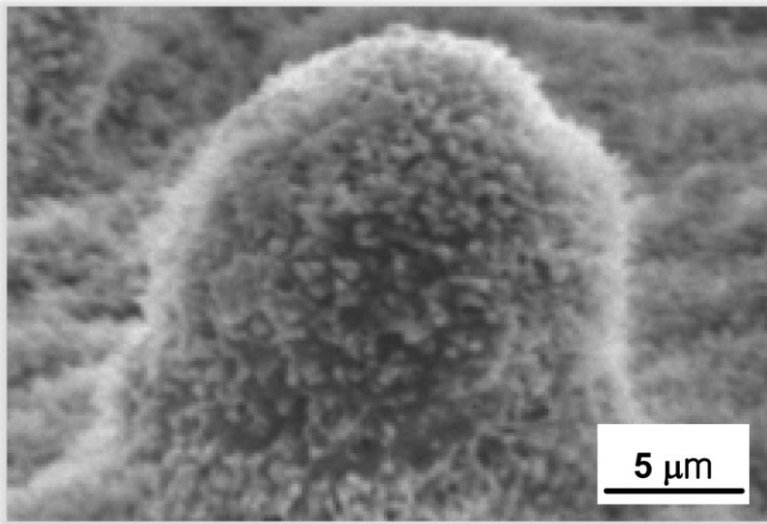
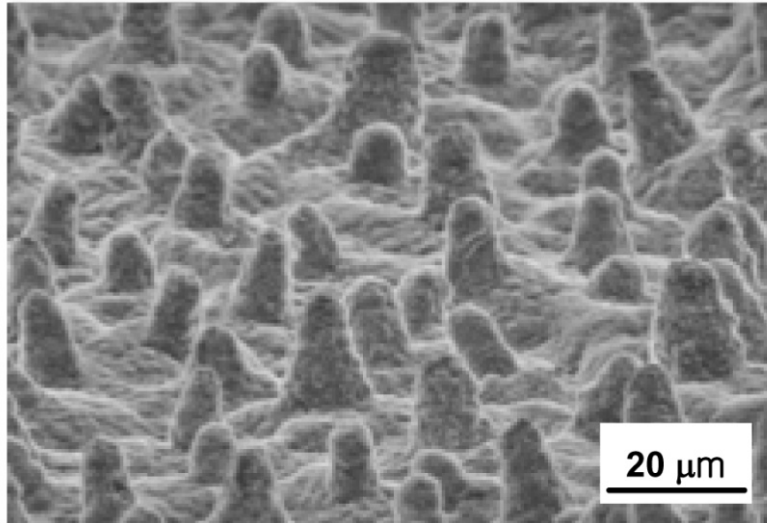


Adhesion measurement in PBS with functionalized tip



Patterned silica surface exhibits higher adhesion compared to unpatterned silica surface. Biotin coated surface exhibits even higher adhesion.

Hierarchical Nanostructures for Superhydrophobicity & self cleaning



Nelumbo nucifera (lotus)

SEM of Lotus leaf showing bump structure.

One of the crucial property in wet environments is non-wetting or superhydrophobicity and self cleaning. These surfaces are of interest in various applications, e.g., self cleaning windows, windshields, exterior paints for buildings, navigation-ships and utensils, roof tiles, textiles and reduction of drag in fluid flow, e. g. in micro/nanochannels. Also, superhydrophobic surface can be used for energy conservation and energy conversion such as in the development of a microscale capillary engine.

Reduction of wetting is also important in reducing meniscus formation, consequently reducing stiction.

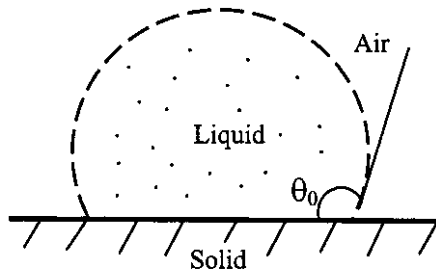
Various natural surfaces, including various leaves, e. g. Lotus, are known to be superhydrophobic, due to high roughness and the presence of a wax coating (Neinhuis and Barthlott, 1997)



Rolling off liquid droplet over superhydrophobic Lotus leaf
with self cleaning ability

Roughness optimization model for superhydrophobic and self cleaning surfaces

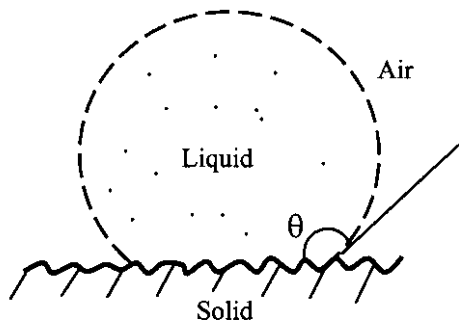
Smooth surface



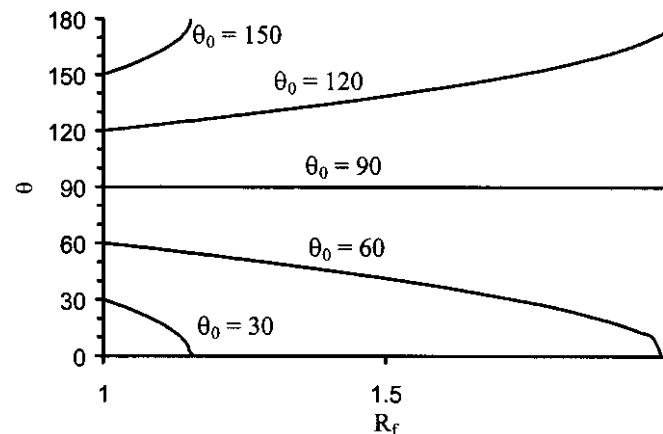
Wenzel's equation:

$$\cos \theta = R_f \cos \theta_o$$

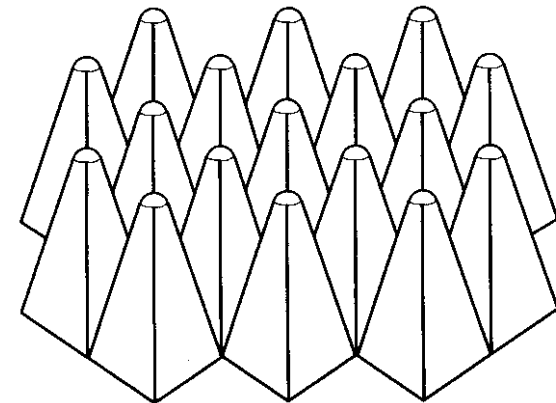
Effect of roughness



Effect of roughness

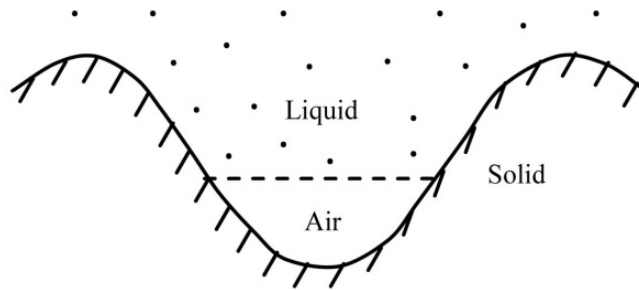


Hemispherically topped pyramidal asperities



Droplet of liquid in contact with a smooth and rough surface Effect of roughness on contact angle

Formation of the composite interface

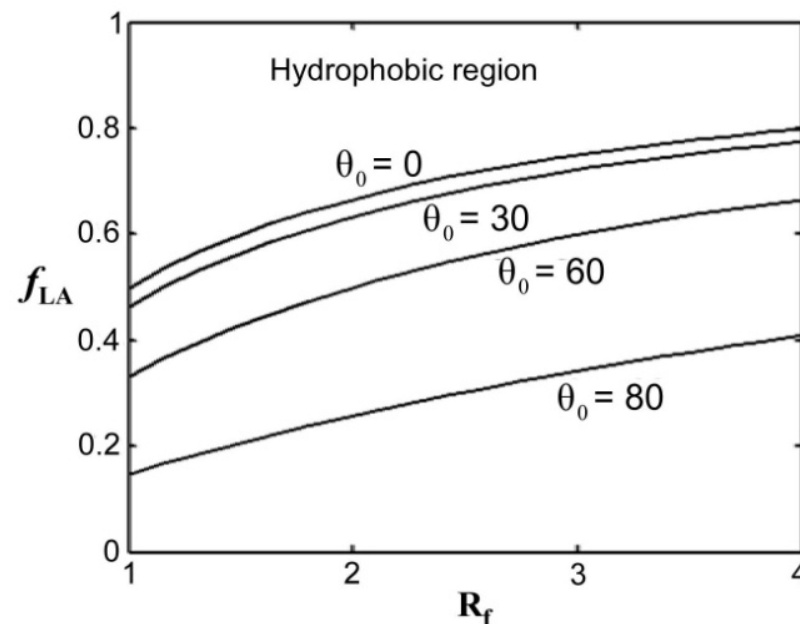


Cassie-Baxter equation:

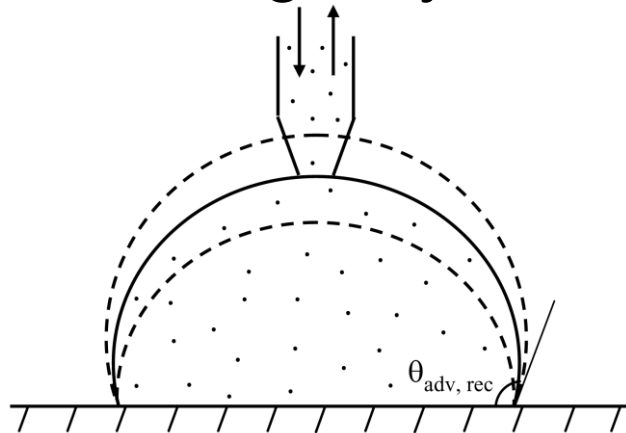
$$\begin{aligned}\cos \theta &= R_f f_{SL} \cos \theta_0 - f_{LA} \\ &= R_f \cos \theta_0 - f_{LA} (R_f \cos \theta_0 + 1)\end{aligned}$$

f_{LA} requirement for a hydrophilic surface to be hydrophobic

$$f_{LA} \geq \frac{R_f \cos \theta_0}{R_f \cos \theta_0 + 1} \quad \text{for } \theta_0 < 90^\circ$$



In fluid flow, another property of interest is contact angle hysteresis (θ_H)

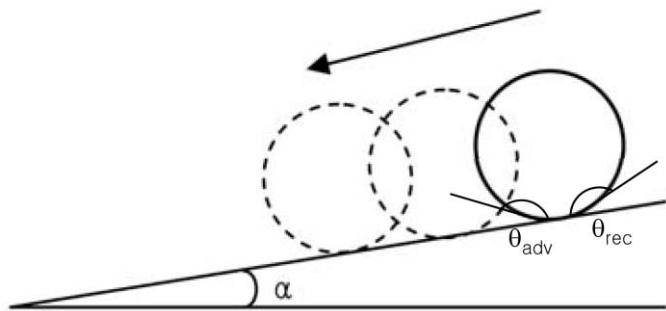


Increased droplet volume $\Rightarrow \theta_{adv}$: Advancing contact angle

Decreased droplet volume $\Rightarrow \theta_{rec}$: Receding contact angle

$$\theta_H = \theta_{adv} - \theta_{rec}$$

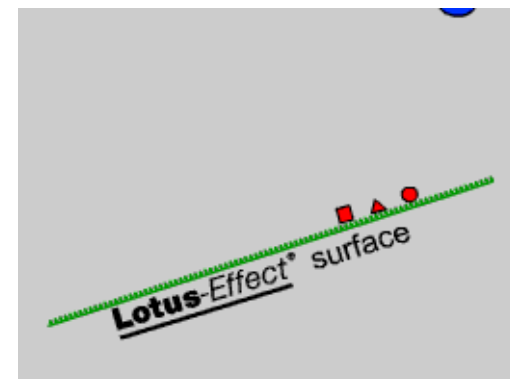
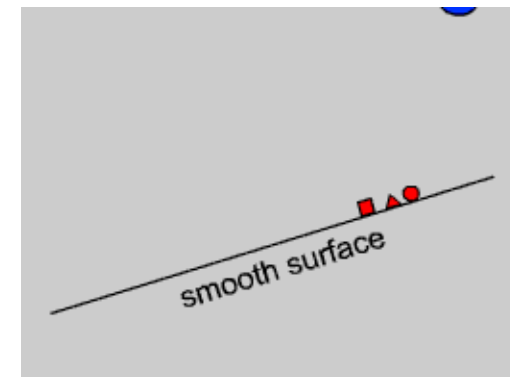
If θ_H is low, energy spent during movement of a droplet is small and a droplet can move easily at a small tilt angle



α : Tilt angle

$$\theta_{adv} - \theta_{rec} \approx \frac{R_f \sqrt{1 - f_{LA}} (\cos \theta_{rec0} - \cos \theta_{adv0})}{\sqrt{2(R_f \cos \theta_0 + 1)}} \quad \text{for high contact angle } (\theta \rightarrow 180^\circ)$$

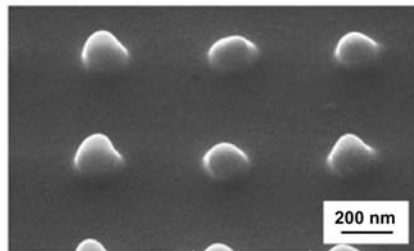
Increase in f_{LA} and reduction in R_f decrease $\theta_{adv} - \theta_{rec}$



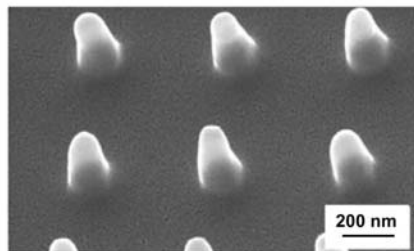
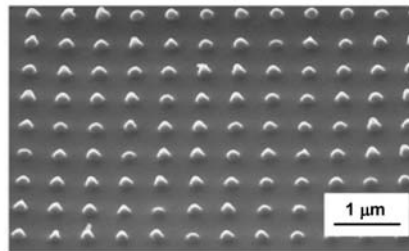
Fabrication and characterization of nanopatterned polymers

Study the effect of nano- and microstructure on superhydrophobicity

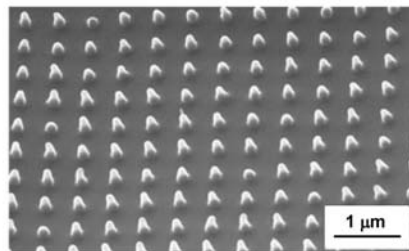
Nanopatterns



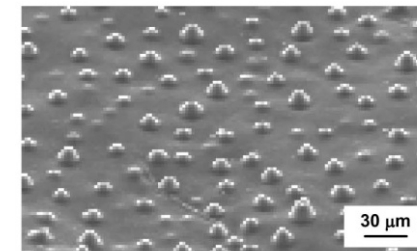
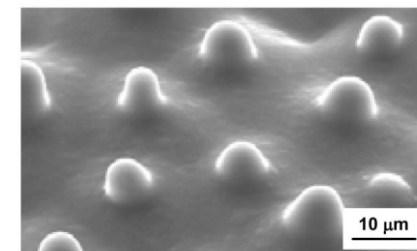
Low aspect ratio (LAR) – 1:1 height to diameter



High aspect ratio (HAR) – 3:1 height to diameter



Micropatterns

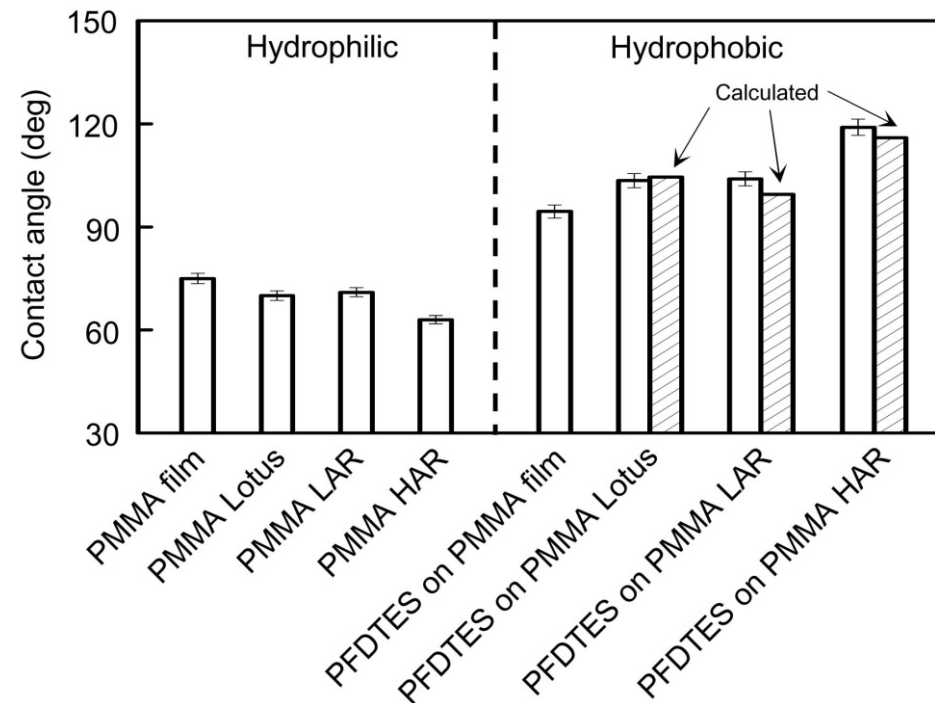


Lotus patterned

- Materials
 - Sample
 - Poly(methyl methacrylate) (PMMA) (hydrophilic) for nanopatterns and micropatterns
 - Hydrophobic coating for PMMA
 - Perfluorodecyltriethoxysilane (PFDTES) (SAM)

Contact angle on micro-/nanopatterned polymers

- Different surface structures: film, Lotus, LAR, HAR
- Hydrophobic film, PFDTES, on PMMA and PS surface structures



	LAR	HAR	Lotus
R_f	2.1	5.6	3.2

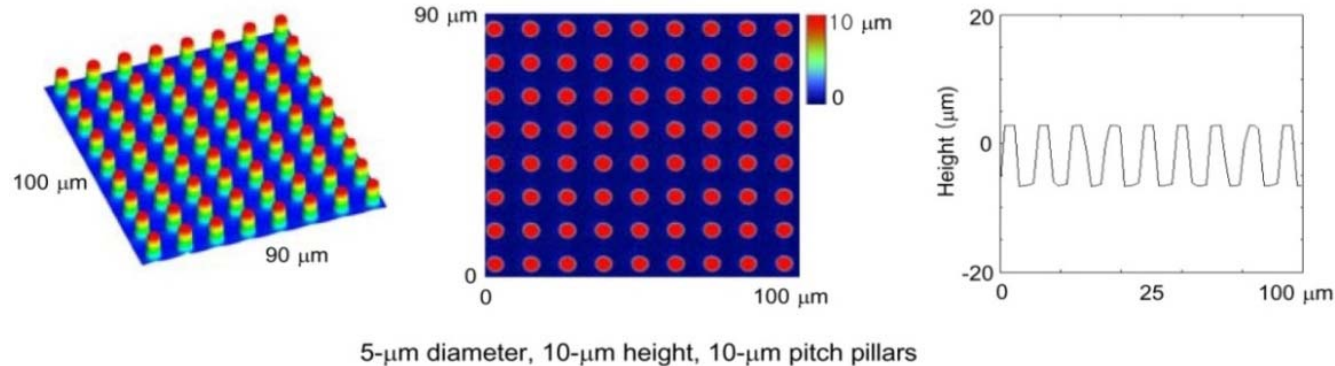
- In hydrophilic surfaces, contact angle decreases with roughness and in hydrophobic surfaces, it increases.
- The measured contact angles of both nanopatterned samples are higher than the calculated values using Wenzel equation. It suggests that nanopatterns benefit from air pocket formation. Furthermore, pinning at top of nanopatterns stabilizes the droplet.

Fabrication and characterization of micropatterned silicon

Transition for Cassie-Baxter to Wenzel regime depends upon the roughness spacing and radius of droplet. It is of interest to understand the role of roughness and radius of the droplet.

Optical profiler surface height maps of patterned Si with PF_3

- Different surface structures with flat-top cylindrical pillars:
 - Diameter (5 μm) and height (10 μm) pillars with different pitch values (7, 7.5, 10, 12.5, 25, 37.5, 45, 60, and 75 μm)



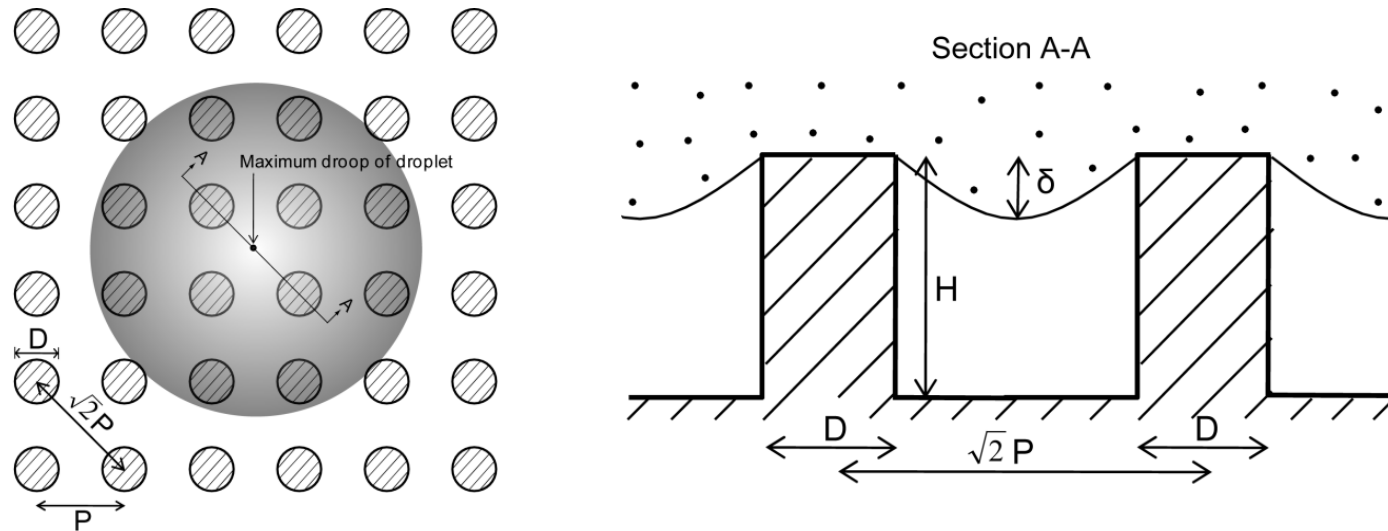
- Materials
 - Sample – Single-crystal silicon (Si)
 - Hydrophobic coating – 1, 1, -2, 2, -tetrahydroperfluorodecyltrichlorosilane (PF_3) (SAM)

B. Bhushan and Y. C. Jung, *Ultramicroscopy* 107, 1033 (2007); *J. Phys.: Condens. Matter* 20, 225010 (2008); B. Bhushan, M. Nosonovsky, and Y. C. Jung, *J. R. Soc. Interf.* 4, 643 (2007); Y. C. Jung, and B. Bhushan, *Scripta Mater.* 57, 1057 (2007); *J. Microsc.* 229, 127 (2008); *Langmuir* 24, 6262 (2008); M. Nosonovsky and B. Bhushan, *Ultramicroscopy* 107, 969 (2007); *Nano Letters* 7, 2633 (2007); *J. Phys.: Condens. Matter* 20, 225009 (2008); *Mater. Sci. Eng.:R* 58, 162 (2007); *Langmuir* 24, 1525 (2008)

Nanoprobe Laboratory for Bio- & Nanotechnology and Biomimetics



Transition criteria for patterned surfaces



- The curvature of a droplet is governed by Laplace eq. which relates pressure inside the droplet to its curvature. The maximum droop of the droplet

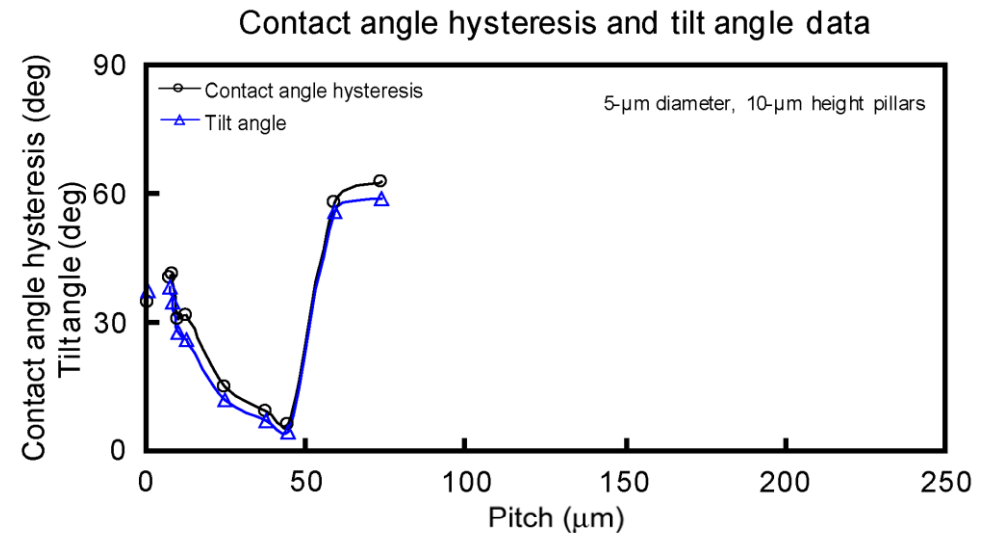
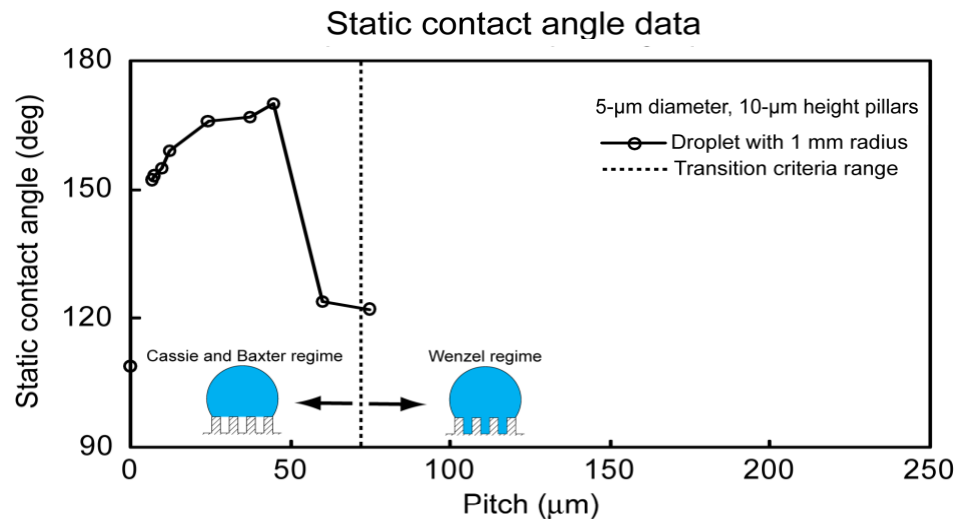
$$\delta \approx \frac{(\sqrt{2}P - D)^2}{R}$$

If $\delta \geq H \implies$ Transition from Cassie-Baxter regime to Wenzel regime

- Geometry (P and H) and radius R govern transition. A droplet with a large radius (R) w.r.to pitch (P) would be in Cassie-Baxter regime.

Contact angle, hysteresis, and tilt angle on patterned Si surfaces with PF_3

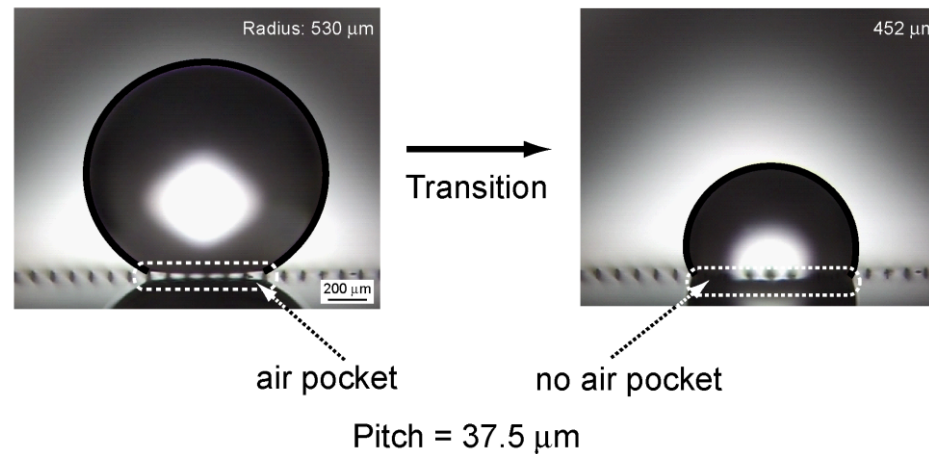
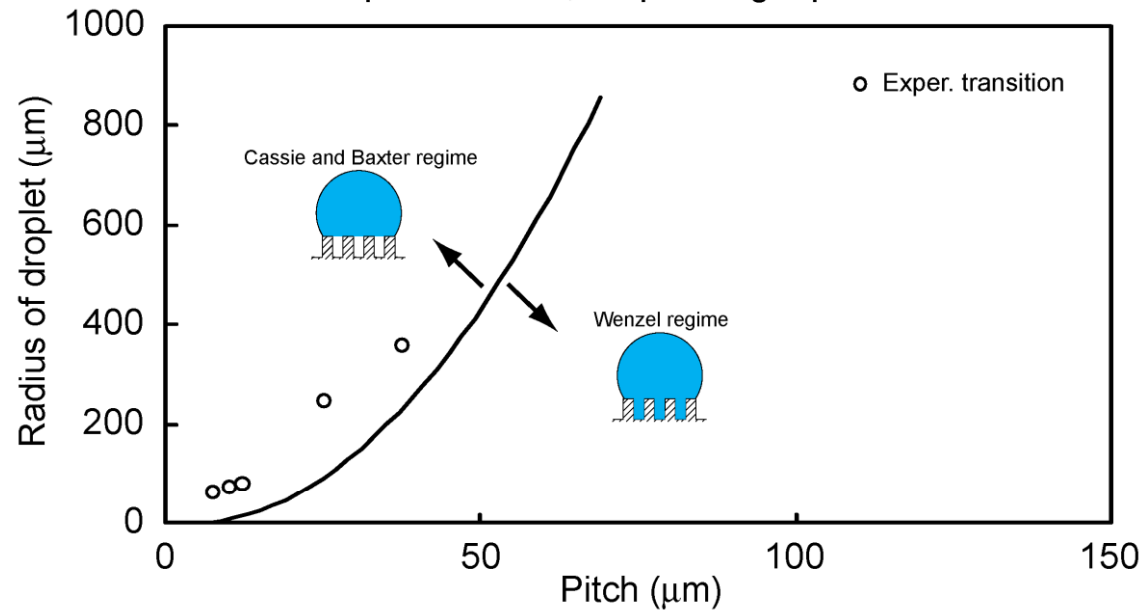
Droplet size = 1 mm in radius



- For the selected droplet, the transition occurs from Cassie-Baxter regime to Wenzel regime at higher pitch values for a given pillar height.

Transition from Cassie-Baxter regime to Wenzel regime

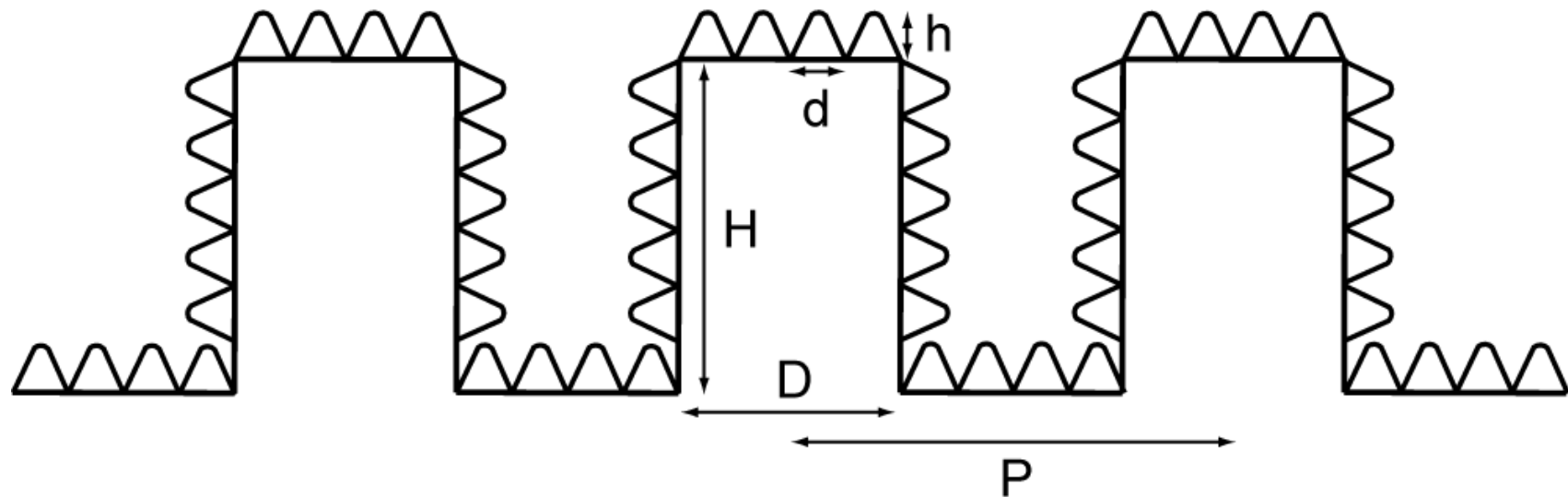
5- μm diameter, 10- μm height pillars



- The critical radius of droplet for the transition increases with the pitch based on both the transition criterion and the experimental data.

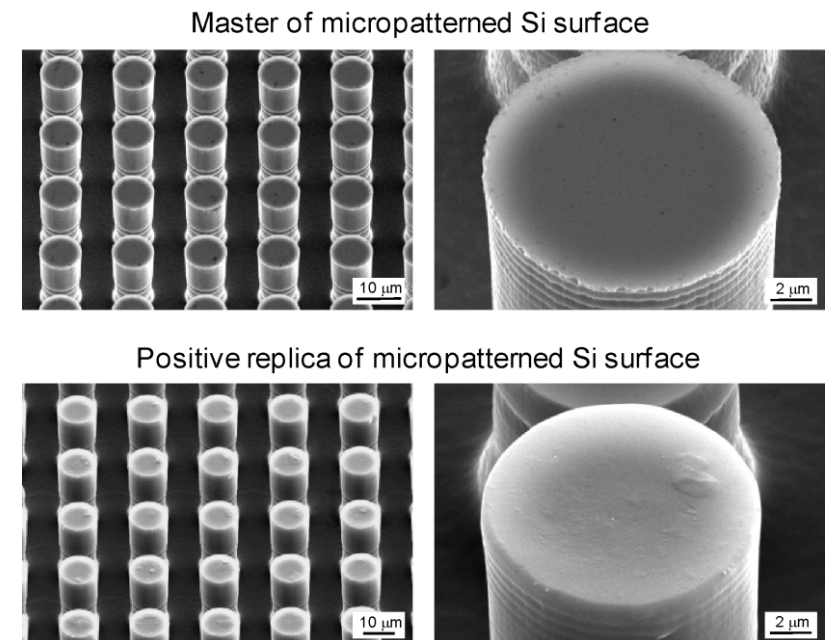
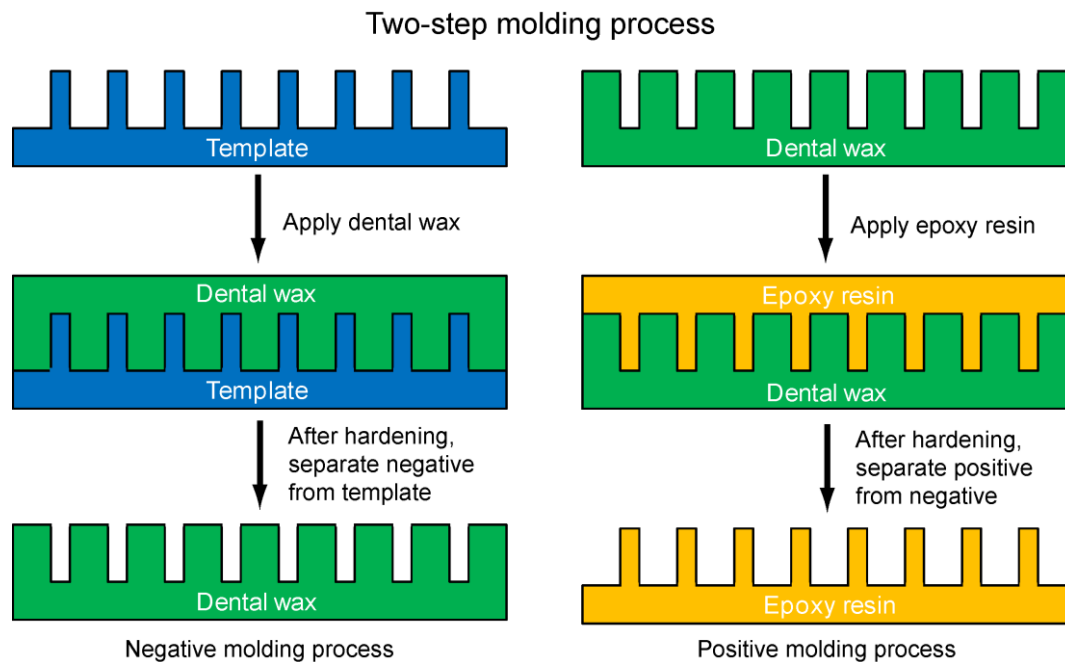
Structure of ideal hierarchical surface

- Based on the modeling and observations made on leaf surfaces, hierarchical surface is needed to develop composite interface with high stability.



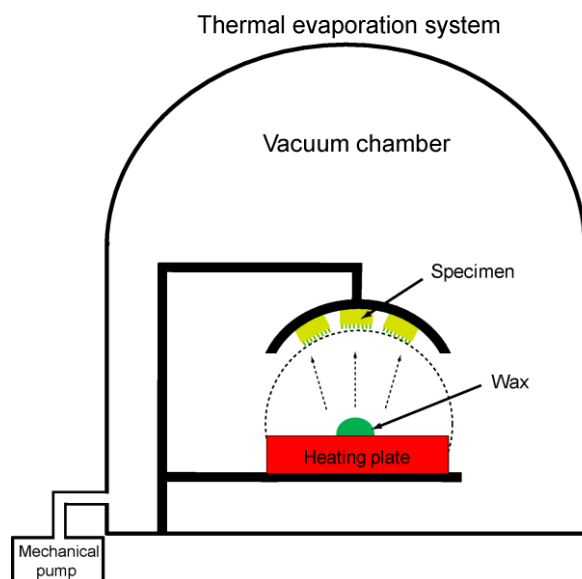
- Proposed transition criteria can be used to calculate geometrical parameters for a given droplet radius. For example, for a droplet on the order of 1 mm or larger, a value of H on the order of 30 μm , D on the order of 15 μm and P on the order of 130 μm is optimum.
- Nanoasperities should have a small pitch to handle nanodroplets, less than 1 mm down to few nm radius. The values of h on the order of 10 nm, d on the order of 100 nm can be easily fabricated.

Fabrication of microstructure

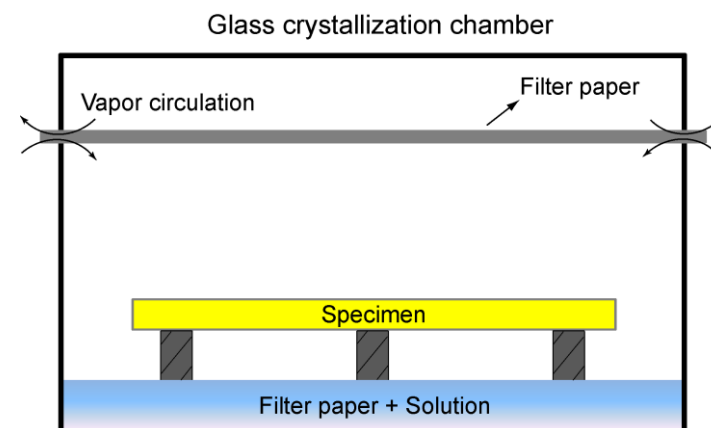
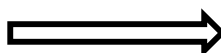


- Microstructure
 - Replication of micropatterned silicon surface using an epoxy resin and then cover with the wax material

Fabrication of nanostructure and hierarchical structure



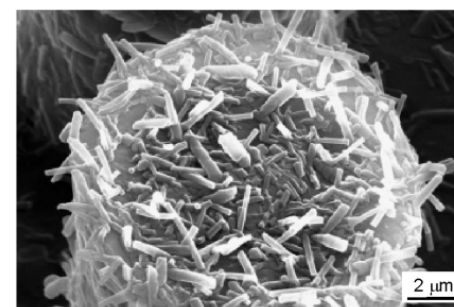
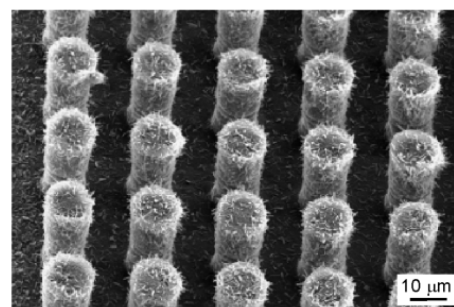
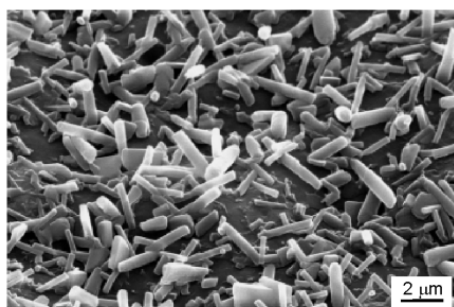
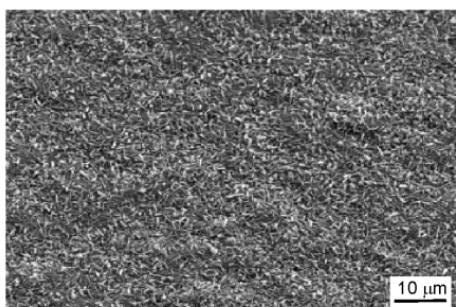
Recrystallization of wax tubules



T. majus wax with ethanol vapor (50° C)

Nanostructure (0.8 $\mu\text{g}/\text{mm}^2$)

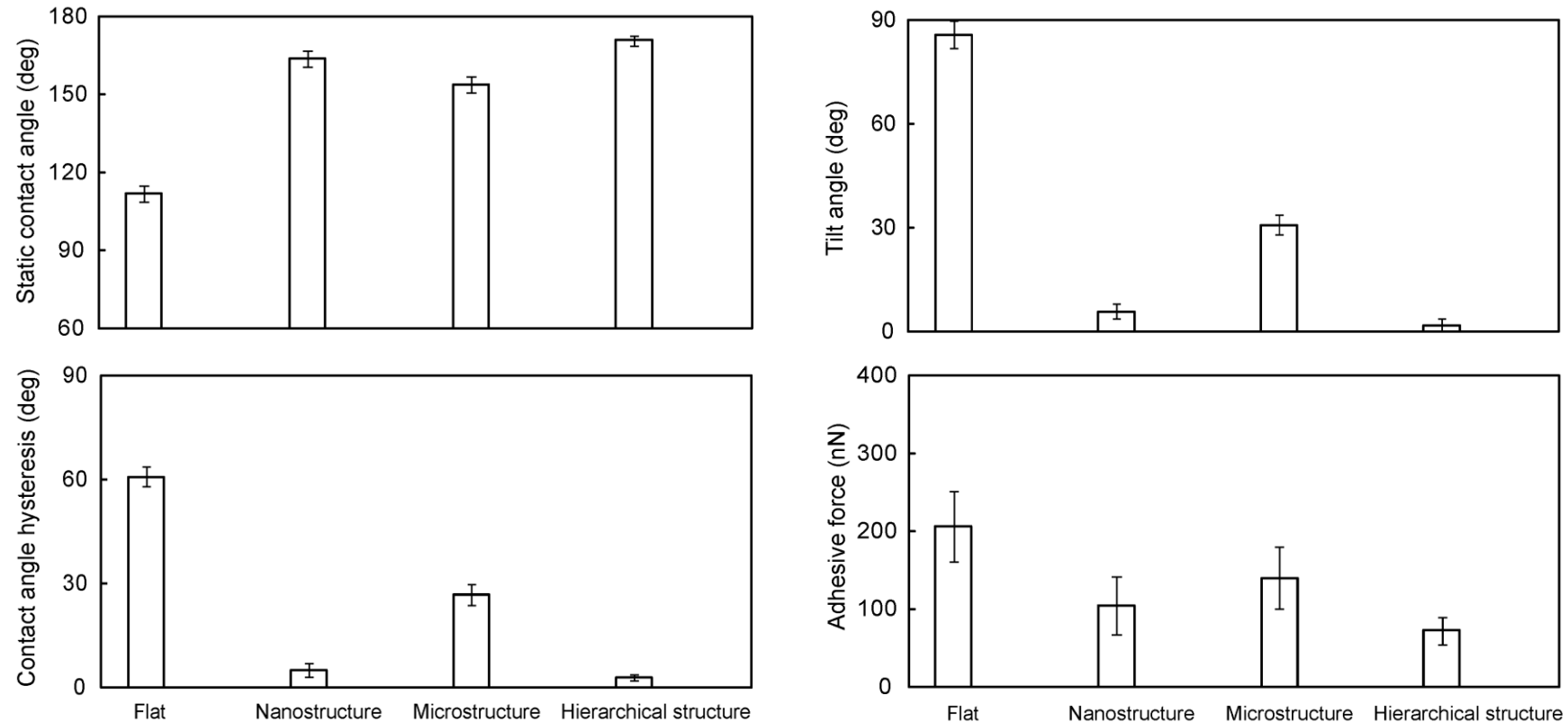
Hierarchical structure (0.8 $\mu\text{g}/\text{mm}^2$)



- Nanostructure
 - Self assembly of the *T. majus* wax deposited by thermal evaporation
 - Expose to a solvent in vapor phase for the mobility of wax molecules
- Hierarchical structure
 - Micropatterned epoxy replica and covered with the tubules of *T. majus* wax

Static contact angle, contact angle hysteresis, tilt angle and adhesive force on various structures

T. majus wax ($0.8 \mu\text{g}/\text{mm}^2$) with ethanol vapor (50°C)



- Nanostructures and hierarchical with tubular wax led to high static contact angle of 160° and 171° and low hysteresis angle on the order of 5° and 2° .
- Hierarchical structure has low adhesive force due to decrease of the solid-liquid contact area in both levels of structuring.

Hierarchical Nanostructures for Reversible Adhesion(Gecko Feet)

Several creatures, including insects, spiders and lizards (e.g., Gecko) have unique ability to cling to ceilings and walls utilizing dry adhesion. They can also detach at will by peeling.

- Gecko is capable of producing 20 N of adhesive force
- This ability is due to the intricate micro/nanostructures that compose the skin of the gecko.
 - Lamellae, Setae, Branches, Spatulae



Gecko

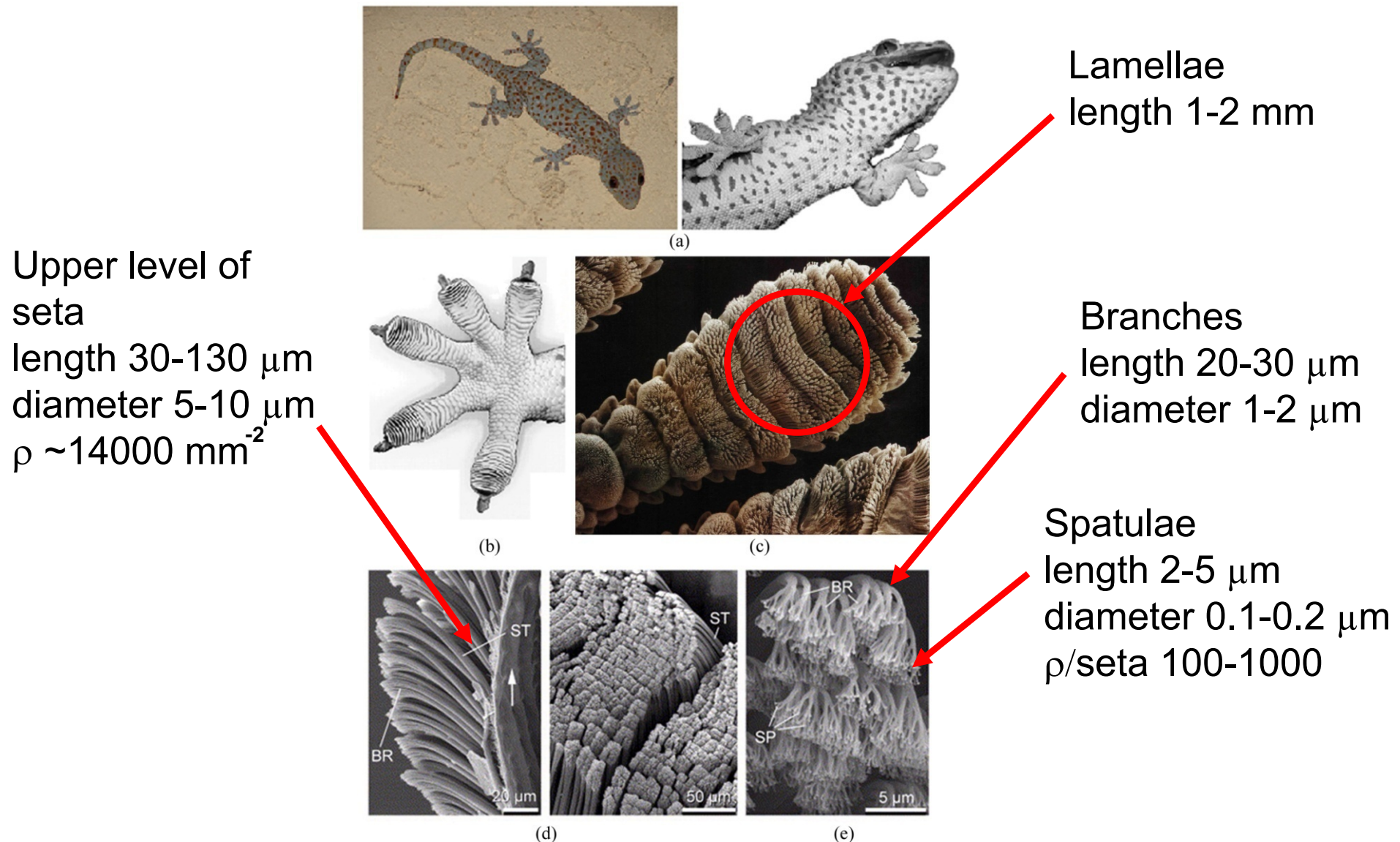


Courtesy MPI Stuttgart

Potential Uses

- Everyday objects
- Adhesive tape, fasteners, and toys
 - MEMS/NEMS
- Wall climbing robots
- Space (microgravity) applications
 - MEMS assembly

Hierarchical structure for adhesion enhancement



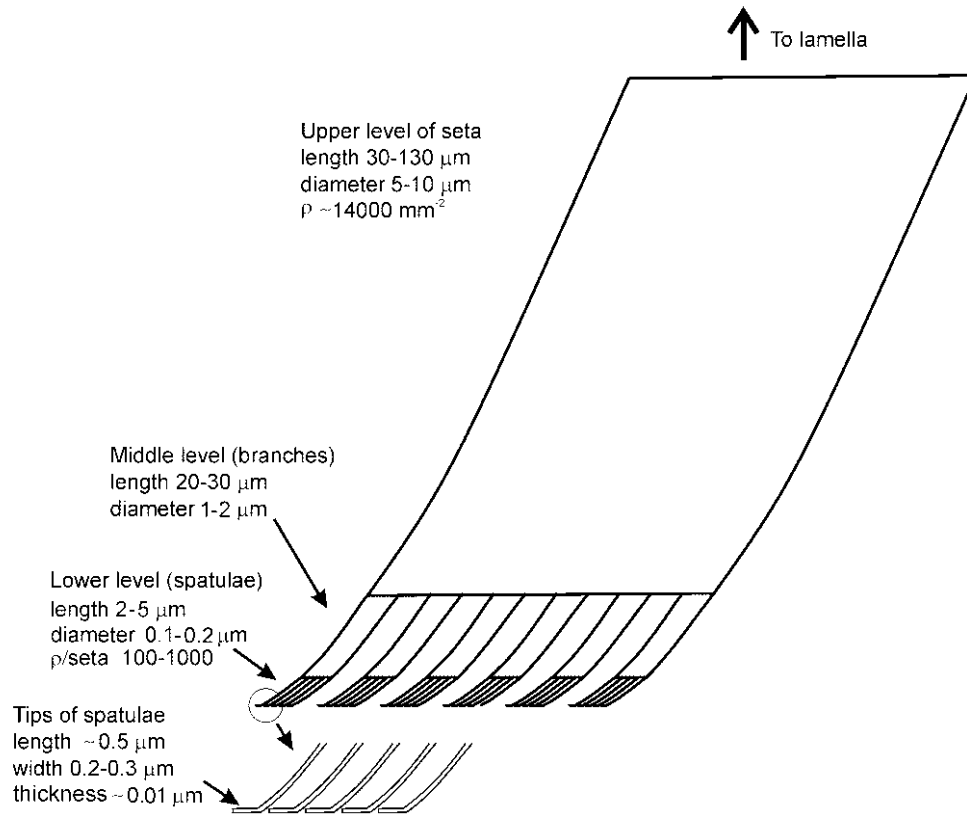
Tokay Gecko Surface Construction

(Autumn et al., 2000; Gao et al., 2005; Autumn, 2006)

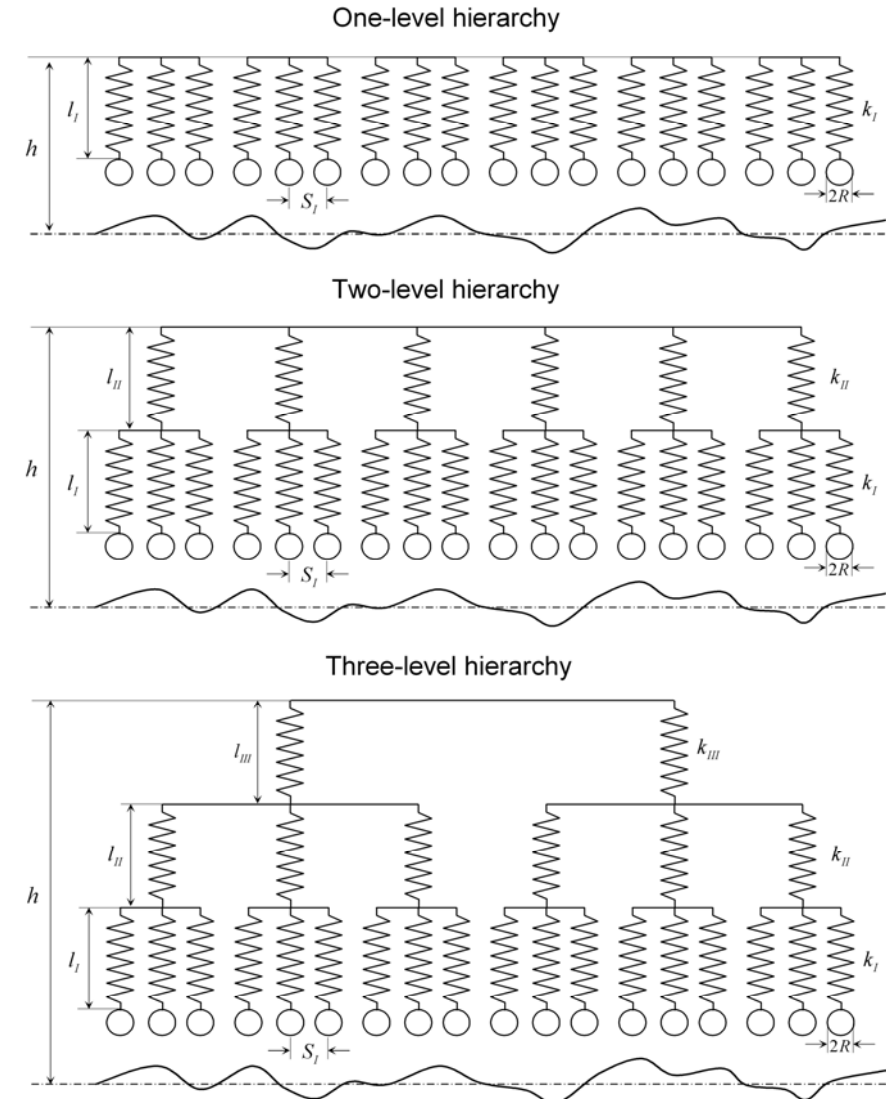
Nanoprobe Laboratory for Bio- & Nanotechnology and Biomimetics



Simulation model



Schematic of three layer hierarchical morphology of gecko seta with three levels of branches: seta level, middle level, and spatula level.



One-, two- and three-level spring models for simulation effect hierarchical morphology on interaction seta with rough surface.

For one-level model, elastic force, F_{el} in the springs (k_I) due to compression of $\Delta\ell$:

$$F_{el} = -k_I \sum_{i=1}^p \Delta l_i u_i \quad u_i = \begin{cases} 1 & \text{if contact} \\ 0 & \text{if no contact} \end{cases}$$

For two-level model,

$$F_{el} = -\sum_{j=1}^q \sum_{i=1}^p k_{ji} (\Delta l_{ji} - \Delta l_j) u_{ji} \quad u_{ji} = \begin{cases} 1 & \text{if contact} \\ 0 & \text{if no contact} \end{cases}$$

For three-level model,

$$F_{el} = -\sum_{k=1}^r \sum_{j=1}^q \sum_{i=1}^p k_{kji} (\Delta l_{kji} - \Delta l_{kj} - \Delta l_j) u_{kji} \quad u_{kji} = \begin{cases} 1 & \text{if contact} \\ 0 & \text{if no contact} \end{cases}$$

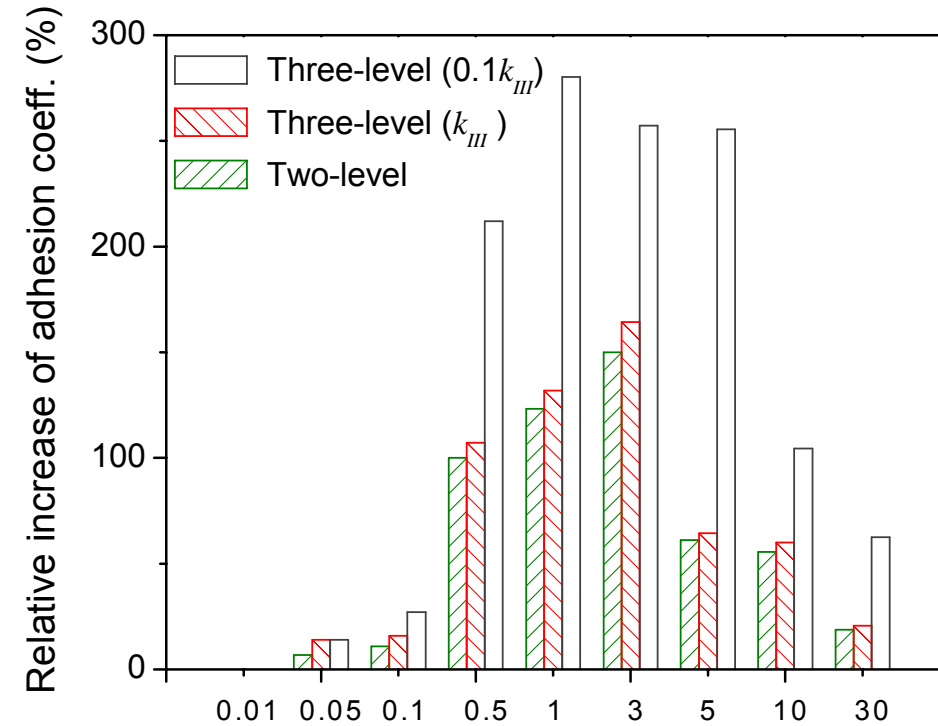
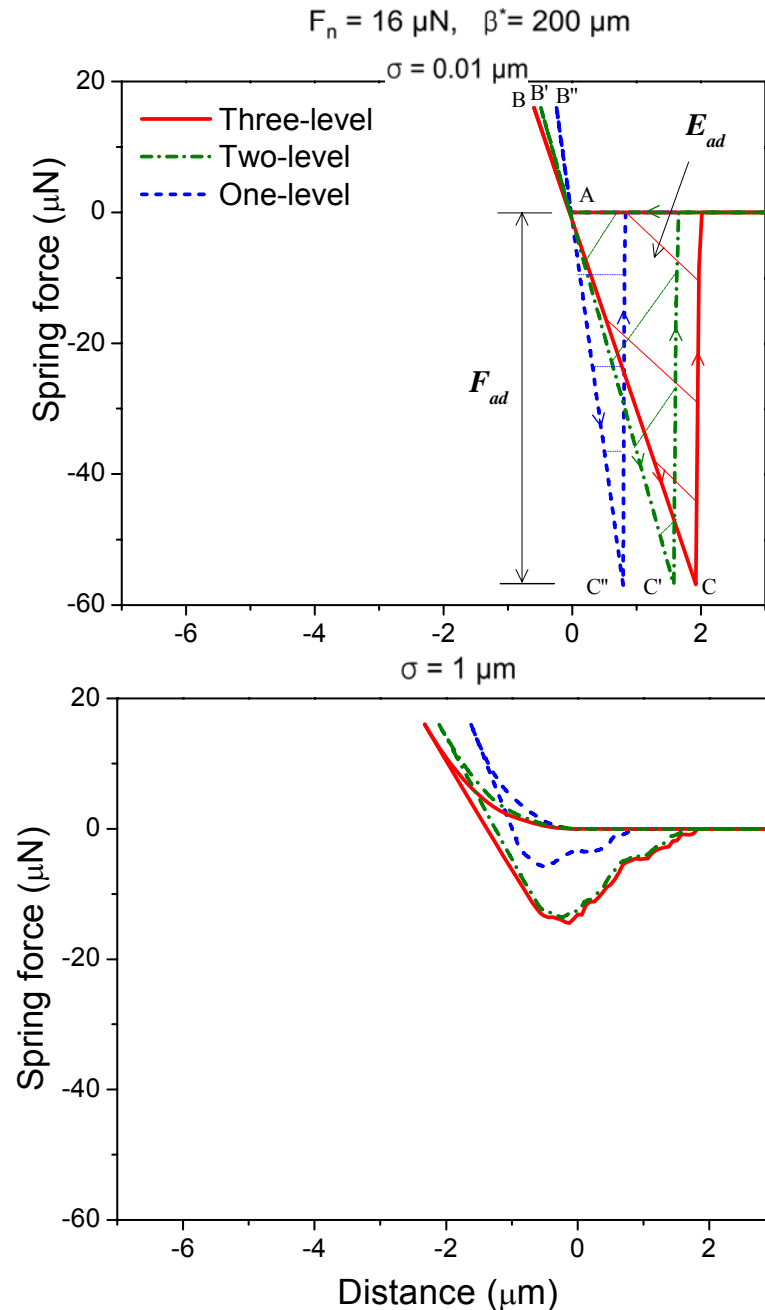
where p , q and r are number of springs in level *I*, *II* and *III* of the model, respectively.

Adhesive force between hemispherical tip of a single spatula of radii R_c with work of adhesion of two surfaces E_{ad} (DMT theory)

$$F_{ad} = 2\pi R_c E_{ad}$$

Springs are pulled away from the surface when the net force (pull off force – attractive adhesive force) at the interface is equal to zero.

The effect of multi-level hierarchical structures on adhesion enhancement



The rate of relative increase for adhesive force a between one- and multi-level models.

Force-distance curves of one-, two- and three-level models in contact with rough surfaces with two different σ values.

Summary of tribology of lubricants, bioadhesion, nanopatterned surfaces and reversible adhesion and device level studies

- **Lubricants for MEMS/NEMS**
 - Bonded PFPE lubricants and SAMs appear to be the best suited for lubrication of MEMS/NEMS
- **Bioadhesion studies**
 - Adhesion between silica surfaces and biomolecules using chemical linker method is stronger than by direct adsorption
- **Nanopatterned surfaces**
 - Optimum roughness distribution can be used to generate superhydrophobic surfaces.
 - Formation of air pockets is desirable. A transition criterion has been proposed.
- **Reversible adhesion (Gecko feet)**
 - Hierarchical structure results in adhesion enhancement.



Acknowledgements

- Financial support has been provided by the National Science Foundation (Contract No. ECS-0301056), the Nanotechnology Initiative of the National Institute of Standards and Technology in conjunction with Nanotribology Research Program (Contract No. 60 NANB1D0071), and Texas Instruments, Intel Corp and Nanochip Inc.
- Polysilicon and SiC work was performed in collaboration with Prof. M. Mehregany and Dr. C. A. Zorman at Case Western Reserve University
- Some of the SAMs were prepared by Drs. P. Hoffmann and H. J. Mathieu at EPFL Lausanne, Switzerland.
- Some of the patterned samples were prepared by Dr. E. Y. Yoon at KIST, Korea and Dr P. Hoffmann at EPFL Lausanne, Switzerland.
- The BioMEMS/BioNEMS studies were carried out in collaboration with Prof. S. C. Lee of OSU Medical School and Prof. D. Hansford of Biomedical Eng.
- DMD chips were supplied by Dr. S. Joshua Jacobs of Texas Instruments



References

- B. Bhushan (1999), *Handbook of Micro/Nanotribology*, second ed. CRC Press, Boca Raton, Florida.
- B. Bhushan (2005), *Nanotribology and Nanomechanics – An Introduction*, Springer-Verlag,
- B. Bhushan (2007), *Springer Nanotechnology Handbook*, 2nd ed., Springer-Verlag, Heidelberg.
- B. Bhushan (2007), “Nanotribology and Nanomechanics of MEMS/NEMS and BioMEMS/BioNEMS Materials and Devices,” *Microelectronic Eng.* **84**, 387-412.
- Bhushan, B., Tokachichu, D. R., Keener, M., and Lee, S. C. (2005), “Morphology and Adhesion of Biomolecules on Silicon Based Surfaces,” *Acta Biomater.*, **1**, 327-341.
- Tokachichu, D. R. and Bhushan, B. (2006), “Bioadhesion of Polymers for BioMEMS,” *IEEE Trans. Nanotech.* **5**, 228-231. .
- Nosonovsky, M. and Bhushan, B. (2005), “Roughness Optimization for Biomimetic Superhydrophobic Surfaces,” *Microsyst. Technol.* **11**, 535-549.
- Burton Z. and Bhushan, B. (2005), “Hydrophobicity, Adhesion and Friction Properties of Nanopatterned Polymers and Scale Dependence for MEMS/NEMS,” *NanoLetters*, **5**, 1607-1613.
- S. Sundararajan and B. Bhushan (2002), “Development of AFM-based techniques to measure mechanical properties of nanoscale structures,” *Sensors and Actuators A* **101**, 338-351.
- H. Liu and B. Bhushan (2004), “Nanotribological Characterization of Digital Micromirror Devices using an Atomic Force Microscope,” *Ultramicroscopy*, **100**, 391-412.
- Kasai, T., Bhushan, B., Kulik, G., Barbieri, L., and Hoffmann, P. (2005), “Nanotribological Study of Perfluorosilane SAMs for Anti-Stiction and Low Wear,” *J. Vac. Sci. Technol. B* **23**, 995-1003.
- Kim, T. W. and Bhushan, B. (2007), “The Adhesion Analysis of Multi-Level Hierarchical Attachment System Contacting with a Rough Surface,” *J. Adhesion Sci. Technol.* **21**, 1-20.

